

Matrix Completion via Nonsmooth Regularization of Fully Connected Neural Networks

Sajad Faramarzi, Farzan Haddadi, Sajjad Amini, Masoud Ahookhosh

Abstract—Conventional matrix completion methods approximate the missing values by assuming the matrix to be low-rank, which leads to a linear approximation of missing values. It has been shown that enhanced performance could be attained by using nonlinear estimators such as deep neural networks. Deep fully connected neural networks (FCNNs), one of the most suitable architectures for matrix completion, suffer from over-fitting due to their high capacity, which leads to low generalizability. In this paper, we control over-fitting by regularizing the FCNN model in terms of the ℓ_1 norm of intermediate representations and nuclear norm of weight matrices. As such, the resulting regularized objective function becomes nonsmooth and nonconvex, i.e., existing gradient-based methods cannot be applied to our model. We propose a variant of the proximal gradient method and investigate its convergence to a critical point. In the initial epochs of FCNN training, the regularization terms are ignored, and through epochs, the effect of that increases. The gradual addition of nonsmooth regularization terms is the main reason for the better performance of the deep neural network with nonsmooth regularization terms (DNN-NSR) algorithm. Our simulations indicate the superiority of the proposed algorithm in comparison with existing linear and nonlinear algorithms.

Index Terms—Matrix completion, nonsmooth regularization terms, over-fitting, proximal operator, DNN-NSR algorithm.

I. INTRODUCTION

MATRIX completion aims at estimating the empty entries of a matrix with partial observations [1], [2], [3], [4], [5], [6], which is widely used in image inpainting [7], [8], wireless sensor networks localization [9], [10], recommender systems [11], [12], etc. There are two significant categories of matrix completion methods: (i) linear estimators using low-rank matrix completion (LRMC) and (ii) nonlinear matrix completion (NLMC).

Rank minimization and matrix factorization (MF) are two examples of LRMC methods. Given an incomplete data matrix $\mathbf{X} \in \mathbb{R}^{m \times n}$, matrix completion problem can be formulated as

$$\min_{\mathbf{M}} \text{rank}(\mathbf{M}) \quad \text{s.t.} \quad \mathbf{M}_{ij} = \mathbf{X}_{ij}, (i, j) \in \Omega, \quad (1)$$

where $\mathbf{M} \in \mathbb{R}^{m \times n}$, Ω is the set of positions of observed entries, and \mathbf{X}_{ij} and \mathbf{M}_{ij} are the (i, j) -th entry of \mathbf{X} and \mathbf{M} . Due to its nonconvexity and discontinuous nature, solving the rank minimization problem given in (1) is NP-hard [1]. Alternatively, the nuclear norm is used as a convex approximation

of the rank function [13], and problem (1) can be translated to

$$\min_{\mathbf{M}} \|\mathbf{M}\|_* \quad \text{s.t.} \quad \mathbf{M}_{ij} = \mathbf{X}_{ij}, (i, j) \in \Omega, \quad (2)$$

where $\|\cdot\|_*$ stands for nuclear norm.

Approaches based on Singular Value Thresholding (SVT) [14] and Inexact Augmented Lagrange Multiplier (IALM) [15] were suggested to deal with (2). In order to have better approximations of the rank function, new extensions were studied in [16], [17]. In addition, the Truncated Nuclear Norm (TNN) method for matrix completion was proposed in [16]. To improve the convergence rate of the TNN method, a Truncated Nuclear Norm Regularization Method based on Weighted Residual Error (TNNWRE) was given in [17].

Rank function and nuclear norm are special cases of the Schatten p -norm with $p = 0$ and $p = 1$, respectively, i.e., smaller values of p are better approximations of the rank function and improve performance in matrix completion [18]. Although, the Schatten p -norm is not convex when $0 < p < 1$, thus finding the global optimizer is not generally guaranteed. On the other hand, common algorithms for minimizing the nuclear norm or the Schatten p -norm cannot scale to large matrices because they need the singular value decomposition (SVD) in every iteration of the optimization [19], [20]. Factored nuclear norm (F-nuclear norm) is a SVD-free method [21], [22]. Adaptive corRelation Learning (NCARL) for the LRMC problem [23] applies a nonconvex surrogate instead of the rank function, which has a faster convergence rate and is solved by closed-form intermediate solutions.

Alternatively, one can apply MF approaches to handle the LRMC problem. Approximating a low-rank matrix $\mathbf{M} \in \mathbb{R}^{m \times n}$ with a matrix product form $\mathbf{M} = \mathbf{AB}$ where $\mathbf{A} \in \mathbb{R}^{m \times r}$ and $\mathbf{B} \in \mathbb{R}^{r \times n}$ with $\text{rank } r < \min(m, n)$ is a more straightforward way than minimizing the nuclear norm. Therefore, the following nonconvex model was proposed in [24]

$$\min_{\mathbf{A}, \mathbf{B}, \mathbf{M}} \|\mathbf{AB} - \mathbf{M}\|_F^2 \quad \text{s.t.} \quad \mathbf{M}_{ij} = \mathbf{X}_{ij}, (i, j) \in \Omega, \quad (3)$$

where $\|\cdot\|_F$ stands for the Frobenius norm. Let us emphasize that linearity is the fundamental assumption in the LRMC methods [25], which covers rank approximation and MF approaches. However, it is notable that the performance of such methods is poor if data comes from a nonlinear nature [26], [27].

In recent years, there has been an interest in applying nonlinear models for matrix completion. As an example, kernelized probabilistic matrix factorization (KPMF) was proposed in [28], where the matrix is assumed to be the product

S. Faramarzi (e-mail: sajad.faramarzi1397@gmail.com) and F. Haddadi (e-mail: farzanhaddadi@iust.ac.ir) are with the School of Electrical Engineering, Iran University of Science & Technology, Tehran, Iran. S. Amini (e-mail: s_amin@sharif.edu) is affiliated with the Electronics Research Institute (ERI) at Sharif University of Technology, Tehran, Iran. Additionally, S. Amini is a Visiting Faculty member at the College of Information and Computer Sciences, University of Massachusetts Amherst, Amherst, MA, USA. M. Ahookhosh (e-mail: masoud.ahookhosh@uantwerp.be) is with Department of Mathematics at the University of Antwerp, Antwerp, Belgium.

of two latent matrices sampled from two different zero-mean Gaussian Processes (GP). Covariance functions of the GPs are derived from side information and create the nonlinear part of the model. The NLMC methods map data into some feature space with linear structures via a nonlinear function. The resulting matrix is low-rank, and minimizing its Schatten p -norm can recover the missing entries [29].

Artificial Neural Network (ANN) is another powerful tool to deal with NLMC, where the missing entries of the matrix are estimated by a nonlinear function that results from a nonlinear activation function. Restricted Boltzmann Machine (RBM), AutoEncoders (AEs), and recurrent neural networks (RNNs) are examples of ANN used for NLMC [30], [31], [32]. Feed-forward neural networks and the multi-layer perceptron (MLP) are of great interest for solving NLMC due to their particular structure [31], [33], [34], [35], [36]. The first AE-based method for NLMC was AutoEncoder-based Collaborative Filtering (AECF) [31]. Missing entries of the matrix are replaced by pre-defined constant and taken by AECF as input. The biases introduced by the pre-defined constants affect the performance of AECF. The modification of AECF with the help of defining the loss function that only considers the outputs corresponding to the input led to the introduction of the AutoEncoder-based Matrix Completion (AEMC) method [33]. Deep Learning-based Matrix Completion (DLMC) is the deep version of AEMC and can outperform shallow methods of matrix completion [33].

Over-fitting is a problem with ANNs that originates from the model's high-representation capacity provided for limited training data. This issue becomes more severe in matrix completion problems in which the training data is an incomplete matrix with minimal available entries. One of the ways to deal with over-fitting is to apply some regularizations to the underlying nonlinear model. In [33], the Frobenius norm of the weight matrices was suggested for regularization. In [34], two AEs were considered, one for row vectors and the other for column vectors. The resulting architecture is regularized using the cosine similarity criterion between the outputs of the code layers. The idea of using Matrix Completion Kernel Regularization (MCKR) comes from a classical perspective, where kernels transfer data points into high-dimensional space that a nonlinear problem is transferred into a linear one [35].

Bi-branch neural networks (BiBNNs) with two independent fully connected neural networks (FCNNs) were introduced for matrix completion [36] using the MF technique. For $\mathbf{M}^{m \times n} = \mathbf{A}^{m \times r} \mathbf{B}^{r \times n}$, $\mathbf{M}_{i,j}$ is created using the i -th row of \mathbf{A} and j -th column of \mathbf{B} as inputs into branches, and $\widehat{\mathbf{M}}_{i,j}$ is estimated using nonlinear transforms. For a nonlinear function $f(\cdot)$, the model $\mathbf{M}^{m \times n} = f(\mathbf{A}) + \mathbf{A}^{m \times r} \mathbf{B}^{r \times n}$ was proposed in [37], applying a neural network with two separate branches. Both branches work to recover the partially observed matrix in multi-task learning with regularization terms.

This paper introduces novel nonsmooth regularizers to deal with over-fitting issues arising in NLMC models, i.e., conventional smooth optimization techniques such as Stochastic Gradient Descent (SGD) can not be used for training. To deal with this issue, the pretraining of AEs with one regularization term for a two-layer FCNN was suggested using proximal

methods in [38]. The approach is extended for training feed-forward neural networks with one nonsmooth regularization term in [39]. Extrapolation of parameters is used to increase the algorithm's convergence rate. We here propose an extrapolated proximal gradient method for training deep neural networks. Our main contributions are summarized as follows:

- We deal with the over-fitting issue of the ANNs by taking advantage of the ℓ_1 norm of the outputs of all hidden layers and the nuclear norm of the weight matrices. These regularization terms control the ANNs parameters which increase the generalizability of the model.
- Our extrapolated proximal gradient method is designed to use the well-known penalty method, i.e., our method gradually adds the effect of the regularization terms to the loss function, improving the ANNs training performance. This is called **gradual learning**.
- We show that conditions needed for any general algorithm in [40] to converge to a critical point are met in our deep neural network model with nonsmooth regularization terms.
- Comparison of the simulation results of the proposed algorithm with two classical algorithms, IALM and NCARI, and three algorithms based on deep neural networks (DNNs), AEMC, DLMC, and BiBNN, show its superiority.

The rest of the paper is organized as follows. The notation and preliminaries are presented in section II. The formulation of the matrix completion problem and previously proposed regularizers are given in Section III. Our proposed method is given in section IV. The experimental results and conclusion are presented in section V and section VI, respectively.

II. NOTATIONS AND PRELIMINARIES

We use bold uppercase and lowercase letters throughout the paper to show matrices and vectors, respectively. The i -th element of vector \mathbf{x} is denoted by x_i , and w_{ij} shows the element of matrix \mathbf{W} at row i and column j . $\text{vec}(\cdot)$ indicates a vectorizing operator that produces column-wise concatenation of the input matrix as output, and $\text{vec}^{-1}(\cdot)$ is the inverse operator. Column-wise and row-wise concatenation of m vectors are denoted by $\mathbf{x} = [\mathbf{x}_1, \dots, \mathbf{x}_m]$ and $\mathbf{y} = [\mathbf{y}_1; \dots; \mathbf{y}_m]$, respectively. $\|\cdot\|_p$ and $\|\cdot\|_F$ indicate the ℓ_p and Frobenius norms, respectively. $\|\cdot\|_1$ is the ℓ_1 vector norm that outputs the sum of the absolute values. $\|\cdot\|_*$ is the nuclear norm of a matrix equal to the sum of its singular values.

Definition 1. (Proximal Operator [41]) : Let $g : \mathbb{R}^n \rightarrow \mathbb{R} \cup \{+\infty\}$ be a proper and lower semi-continuous function. For $\alpha\mu > 0$, the proximal operator $\text{Prox}_{\alpha\mu f} : \mathbb{R}^n \rightarrow \mathbb{R}^n$ of $g(\mathbf{x}) = \alpha\mu f(\mathbf{x})$ is defined as: $\text{Prox}_g(\mathbf{x}) = \arg \min_{\mathbf{y}} (\alpha f(\mathbf{y}) + \frac{1}{2\mu} \|\mathbf{y} - \mathbf{x}\|^2)$.

We can calculate the proximal operator for different functions based on the above definition.

Lemma 1. (Proximal operator for ℓ_1 norm [42]): The proximal operator of $g(\mathbf{x}) = \alpha \|\mathbf{x}\|_1$ is the soft-thresholding function defined as.

$$[\text{Prox}_g(\mathbf{x})]_i = \begin{cases} x_i - \alpha, & \text{if } x_i > \alpha, \\ 0, & \text{if } |x_i| < \alpha, \\ x_i + \alpha, & \text{if } x_i < -\alpha. \end{cases} \quad (4)$$

Definition 2. (Singular value shrinkage operator [14]): Consider the SVD of a matrix $\mathbf{X} \in \mathbb{R}^{m \times n}$, i.e.,

$$\mathbf{X} = \mathbf{U}\mathbf{\Sigma}\mathbf{V}^T, \quad \mathbf{\Sigma} = \text{diag}(\{\sigma_i\}_{1 \leq i \leq \min(m,n)}). \quad (5)$$

Define the singular value shrinkage operator \mathbf{D}_τ as

$$\mathbf{D}_\tau(\mathbf{X}) = \mathbf{U}\mathbf{\Sigma}_\tau\mathbf{V}^T, \quad \mathbf{\Sigma}_\tau = \text{diag}(\max\{\sigma_i - \tau, 0\}). \quad (6)$$

Lemma 2. (Proximal operator for nuclear-norm [14]): The proximal operator of $g(\mathbf{X}) = \beta\|\mathbf{X}\|_*$ is given by

$$\text{Prox}_g(\mathbf{X}) = \mathbf{D}_\beta(\mathbf{X}). \quad (7)$$

Lemma 3 (Proximal operator for ℓ_∞ norm [38]). The proximal operator of $r_\theta(\boldsymbol{\theta})$ is denoted by $\mathbf{u} = \text{Prox}_{\mu_{\theta,k}, r_\theta}(\boldsymbol{\theta})$ for $\mu_{\theta,k} > 0$. $r_\theta(\boldsymbol{\theta})$ is defined as

$$r_\theta(\boldsymbol{\theta}) = \begin{cases} 0, & \|\boldsymbol{\theta}\|_\infty \leq M, \\ \infty, & \|\boldsymbol{\theta}\|_\infty \geq M, \end{cases} \quad (8)$$

where $\|\boldsymbol{\theta}\|_\infty = \max_i |\theta_i|$ and M is a large but bounded value.

$$u_i = \begin{cases} \theta_i, & \text{if } \theta_i \leq M, \\ M\text{sign}(\theta_i), & \text{if } \theta_i > M. \end{cases} \quad (9)$$

Definition 3. (L -smooth functions [40]): A function $f: \mathbb{R}^n \rightarrow \mathbb{R}$ is called L -smooth if there exists $L > 0$ such that

$$\|\nabla f(\mathbf{x}) - \nabla f(\mathbf{y})\| \leq L\|\mathbf{x} - \mathbf{y}\|, \quad \forall \mathbf{x}, \mathbf{y} \in \mathbb{R}^n.$$

Lemma 4. Let $f: \mathbb{R}^n \rightarrow \mathbb{R}$ be a twice continuously differentiable function ($f \in \mathcal{C}^2$) and let \mathcal{C} be a convex compact set. Then, f is L -smooth for some $L > 0$.

Proof. Since $f \in \mathcal{C}^2$, there exists $L > 0$ such that $\|\nabla^2 f(\mathbf{z})\| \leq L$ for any $\mathbf{z} \in \mathcal{C}$. For all $\mathbf{x}, \mathbf{y} \in \mathcal{C}$ and $\tau \in [0, 1]$, the convexity of \mathcal{C} implies $\tau\mathbf{x} + (1-\tau)\mathbf{y} \in \mathcal{C}$. Then, it follows from the mean value theorem that

$$\begin{aligned} \|\nabla f(\mathbf{x}) - \nabla f(\mathbf{y})\| &\leq \int_0^1 \|\nabla^2 f(\tau\mathbf{x} + (1-\tau)\mathbf{y})\| \|\mathbf{x} - \mathbf{y}\| d\tau \\ &\leq L\|\mathbf{x} - \mathbf{y}\|, \end{aligned} \quad (10)$$

which is our desired result. \square

Lemma 5. (Descent Lemma [43]): Let $f: \mathbb{R}^n \rightarrow \mathbb{R}$ be a function and let $\mathcal{C} \subseteq \mathbb{R}^n$ be convex with nonempty interior. Assume that f is continuously differentiable on a neighborhood of each point in \mathcal{C} and L -smooth on \mathcal{C} with $L > 0$. Then, for every two points \mathbf{x} and \mathbf{y} in \mathcal{C} , it holds that

$$f(\mathbf{y}) \leq f(\mathbf{x}) + \nabla^T f(\mathbf{x})(\mathbf{y} - \mathbf{x}) + \frac{L}{2}\|\mathbf{y} - \mathbf{x}\|^2. \quad (11)$$

Lemma 6. Let \mathbf{x} , \mathbf{y} and \mathbf{z} be arbitrary vectors in \mathbb{R}^n . Then

$$\|\mathbf{x} - \mathbf{z}\|^2 - \|\mathbf{y} - \mathbf{z}\|^2 = 2(\mathbf{x} - \mathbf{y})^T(\mathbf{y} - \mathbf{z}) + \|\mathbf{x} - \mathbf{y}\|^2. \quad (12)$$

Lemma 7. (Young's inequality [44]): For $\epsilon > 0$ we have

$$ab \leq \frac{a^2}{2\epsilon} + \frac{\epsilon b^2}{2}. \quad (13)$$

Definition 4. (Fermat rule and critical points [45]): A point \mathbf{x}^* is called a critical point of f if $\mathbf{0} \in \partial f(\mathbf{x}^*)$, where $\partial f(\mathbf{x}^*)$

is the limiting subdifferential at \mathbf{x}^* .

The subsequence convergence analysis in the proposed algorithm for iterations can be extended to the entire sequence using Kurdyka-Łojasiewicz property.

Definition 5. (Kurduka-Łojasiewicz (KL) property [46]): A function $f(\mathbf{x})$ satisfies the KL property at point $\bar{\mathbf{x}} \in \text{dom}(\partial f)$ if there exist $\eta > 0$, a neighborhood $\mathcal{B}_\rho(\bar{\mathbf{x}}) \triangleq \{\mathbf{x} : \|\mathbf{x} - \bar{\mathbf{x}}\| < \rho\}$, and a concave function $g(a) = ca^{1-\theta}$ for some $c > 0$ and $\theta \in [0, 1)$ such that the KL inequality holds

$$g(|f(\mathbf{x}) - f(\bar{\mathbf{x}})|) \text{dist}(\mathbf{0}, \partial f(\mathbf{x})) \geq 1,$$

$$\forall \mathbf{x} \in \mathcal{B}_\rho(\bar{\mathbf{x}}) \cap \text{dom}(\partial f) \text{ and } f(\bar{\mathbf{x}}) < f(\mathbf{x}) < f(\bar{\mathbf{x}}) + \eta, \quad (14)$$

where $\text{dom}(\partial f) = \{\mathbf{x} | \partial f(\mathbf{x}) \neq \emptyset\}$ and $\text{dist}(\mathbf{0}, \partial f(\mathbf{x})) = \min\{\|\mathbf{v}\|_2 | \mathbf{v} \in \partial f(\mathbf{x})\}$ shows the vector in $\partial f(\mathbf{x})$ with the minimum ℓ_2 norm.

III. PRIOR ART

Deep AE, an FCNN with $p - 1$ hidden layers, can be employed to deal with matrix completion problem [33]. Let $\mathbf{X} = [\mathbf{x}_1, \dots, \mathbf{x}_n] \in \mathbb{R}^{m \times n}$ be the partially observed matrix with column \mathbf{x}_i ($i = 1, \dots, n$), which is treated as an input in this architecture. The number of input and output neurons is m (number of rows in matrix \mathbf{X}). For input \mathbf{x}_q , output is given by

$$\hat{\mathbf{x}}_q = g^{(p)}\left(\mathbf{W}^{(p)}\left(\dots\left(g^{(1)}\left(\mathbf{W}^{(1)}\mathbf{x}_q + \mathbf{b}^{(1)}\right)\right)\dots\right) + \mathbf{b}^{(p)}\right), \quad (15)$$

where $q = 1, \dots, n$, while $g^{(i)}$, $\mathbf{b}^{(i)}$, and $\mathbf{W}^{(i)}$ for $i = 1, \dots, p$ is the activation function, bias vectors, and weight matrices, respectively [33]. The vector $\hat{\mathbf{x}}_q$ is a function of network parameters, i.e.,

$$\hat{\mathbf{x}}_q = F_1(\mathbf{W}^{(1)}, \dots, \mathbf{W}^{(p)}, \mathbf{b}^{(1)}, \dots, \mathbf{b}^{(p)}; \mathbf{x}_q). \quad (16)$$

To simplify the notation, vector parameter $\boldsymbol{\theta}$ is defined as

$$\boldsymbol{\theta} = [\text{vec}(\mathbf{W}^{(1)}), \dots, \text{vec}(\mathbf{W}^{(p)}), \mathbf{b}^{(1)}, \dots, \mathbf{b}^{(p)}]. \quad (17)$$

The mean square error (MSE) is usually used as the loss function for the matrix completion problem, i.e.,

$$\ell(\boldsymbol{\theta}) = \frac{1}{n} \sum_{q=1}^n \|\mathbf{x}_q - \hat{\mathbf{x}}_q\|^2. \quad (18)$$

Since the data matrix \mathbf{X} is partially observed, the minimization of (18) is intractable. The binary matrix $\mathbf{N} \in \{0, 1\}^{m \times n}$ is defined as

$$n_{ij} = \begin{cases} 1, & (i, j) \in \Omega, \\ 0, & (i, j) \notin \Omega, \end{cases} \quad (19)$$

Using a column of \mathbf{N} , \mathbf{n}_i ($1 \leq i \leq n$), in (18), a loss function is obtained, which only includes observed elements [31], i.e.,

$$\ell(\boldsymbol{\theta}) = \frac{1}{n} \sum_{q=1}^n \left\| \mathbf{n}_q \odot (\mathbf{x}_q - \hat{\mathbf{x}}_q) \right\|^2, \quad (20)$$

where \odot denotes the Hadamard product. For a regularization hyper-parameter $\lambda > 0$, the over-fitting of FCNNs can be controlled by a regularized objective

$$\ell(\boldsymbol{\theta}) = \frac{1}{n} \sum_{q=1}^n \left\| \mathbf{n}_q \odot (\mathbf{x}_q - \widehat{\mathbf{x}}_q) \right\|^2 + \lambda \sum_{i=1}^p \left\| \mathbf{W}^{(i)} \right\|_F^2, \quad (21)$$

with matrix form

$$\mathcal{L}(\boldsymbol{\theta}) = \left\| \mathbf{N} \odot (\mathbf{X} - \widehat{\mathbf{X}}) \right\|_F^2 + \lambda \sum_{i=1}^p \left\| \mathbf{W}^{(i)} \right\|_F^2, \quad (22)$$

in which $\widehat{\mathbf{X}} = [\widehat{\mathbf{x}}_1, \widehat{\mathbf{x}}_2, \dots, \widehat{\mathbf{x}}_n]$. Next, this regularized loss function needs to be optimized with respect to $\boldsymbol{\theta}$ as

$$\min_{\boldsymbol{\theta}} \mathcal{L}(\boldsymbol{\theta}), \quad (23)$$

where the missing entries of \mathbf{X} are obtained by

$$x_{ij} = \widehat{x}_{ij}, \quad (i, j) \notin \Omega, \quad (24)$$

see [33] for more details.

It is known that applying a regularization term using the ℓ_0 norm on the hidden layers of AE can reduce the generalization error [42]. Moreover, empirical observations have shown that low-rank weight matrices can speed up learning [47] and improve the accuracy, robustness [48], and computational efficiency [49] of DNNs.

IV. PROPOSED MODEL AND METHOD

One can add the rank function of weight matrices in FCNNs and the ℓ_0 pseudo-norm of the outputs of hidden layers to the loss function mentioned in (22). Due to the NP-hardness of the rank minimization and discontinuous nature of the ℓ_0 pseudo-norm, we suggest generating a new model by replacing them with nuclear and ℓ_1 norms, respectively. The resulting model involves convex nonsmooth regularizers [16], [38], and the corresponding optimization problem can be handled efficiently by alternative minimization techniques. The proposed algorithm is a penalty method, where we first train the FCNN with gradually increasing regularization terms.

Our proposed loss function for training l -layers FCNNs involves a simultaneous regularization of the rank of weight matrices and sparsity of the hidden layers, i.e.,

$$\min_{\boldsymbol{\theta}} \mathcal{L}(\boldsymbol{\theta}) + \sum_{q=1}^n \sum_{i=1}^l \alpha_i \left\| \mathbf{z}_q^{(i)} \right\|_0 + \sum_{j=1}^{l+1} \beta_j \text{rank}(\mathbf{W}^{(j)}), \quad (25)$$

where $\mathbf{z}_q^{(i)} = F_2(\mathbf{W}^{(1)}, \mathbf{b}^{(1)}, \dots, \mathbf{W}^{(i)}, \mathbf{b}^{(i)}; \mathbf{x}_q)$ is the output of the i -th hidden layer for the q -th training data, i.e.,

$$\mathbf{z}_q^{(i)} = g^{(i)} \left(\mathbf{W}^{(i)} \left(\dots \left(g^{(1)}(\mathbf{W}^{(1)} \mathbf{x}_q + \mathbf{b}^{(1)}) \right) \dots \right) + \mathbf{b}^{(i)} \right). \quad (26)$$

By approximating the ℓ_0 pseudo-norm with the ℓ_1 norm and the rank function with the nuclear norm in (26), we arrive to

$$\mathcal{P} : \min_{\boldsymbol{\theta}} \mathcal{L}(\boldsymbol{\theta}) + \sum_{q=1}^n \sum_{i=1}^l \alpha_i \left\| \mathbf{z}_q^{(i)} \right\|_1 + \sum_{j=1}^{l+1} \beta_j \left\| \mathbf{W}^{(j)} \right\|_*. \quad (27)$$

At the first step, we add new slack variables $\{\mathbf{h}_q^{(i)}\}_{q=1}^n \Big|_{i=1}^l$ and $\{\mathbf{V}^{(j)}\}_{j=1}^{l+1}$ to the problem as

$$\min_{\mathcal{X}} \mathcal{L}(\boldsymbol{\theta}) + \sum_{q=1}^n \sum_{i=1}^l \alpha_i \left\| \mathbf{h}_q^{(i)} \right\|_1 + \sum_{j=1}^{l+1} \beta_j \left\| \mathbf{V}^{(j)} \right\|_*, \quad (28a)$$

$$\text{s.t. } C1 : \mathbf{h}_q^{(i)} = \mathbf{z}_q^{(i)}, \quad i = 1, \dots, l; q = 1, \dots, n, \quad (28b)$$

$$C2 : \mathbf{V}^{(j)} = \mathbf{W}^{(j)}, \quad j = 1, \dots, l+1, \quad (28c)$$

where $\mathcal{X} = \{\boldsymbol{\theta}, \{\mathbf{h}_q^{(i)}\}_{q=1}^n \Big|_{i=1}^l, \{\mathbf{V}^{(j)}\}_{j=1}^{l+1}\}$. An approximated solution of (28) can be computed via the penalty model

$$\begin{aligned} \min_{\mathcal{X}} \mathcal{L}(\boldsymbol{\theta}) + \sum_{q=1}^n \sum_{i=1}^l \left[\alpha_i \left\| \mathbf{h}_q^{(i)} \right\|_1 + \frac{1}{2\mu_{h^{(i)}}} \left\| \mathbf{z}_q^{(i)} - \mathbf{h}_q^{(i)} \right\|^2 \right] \\ + \sum_{j=1}^{l+1} \beta_j \left[\left\| \mathbf{V}^{(j)} \right\|_* + \frac{1}{2\mu_{v^{(j)}}} \left\| \mathbf{W}^{(j)} - \mathbf{V}^{(j)} \right\|_F^2 \right], \end{aligned} \quad (29)$$

where $\mu_{h^{(i)}} > 0$, $i = 1, \dots, l$ and $\mu_{v^{(j)}} > 0$, $j = 1, \dots, l+1$ are penalty parameters. If we represent the solution to (29) by $\boldsymbol{\theta}^{(\mu_{h^{(i)}}, \mu_{v^{(j)}})}$ and the solution to \mathcal{P} by $\boldsymbol{\theta}^*$, then

$$\lim_{\{\mu_{h^{(i)}}\}_{i=1}^l, \{\mu_{v^{(j)}}\}_{j=1}^{l+1} \rightarrow 0} \boldsymbol{\theta}^{(\mu_{h^{(i)}}, \mu_{v^{(j)}})} = \boldsymbol{\theta}^*. \quad (30)$$

For convergence purposes, we constrain $\boldsymbol{\theta}$ in (29) using $r_{\theta}(\boldsymbol{\theta})$ (defined in (8)). This consequently leads to the minimization problem

$$\begin{aligned} \min_{\mathcal{X}} \mathcal{L}(\boldsymbol{\theta}) + \underbrace{\sum_{q=1}^n \sum_{i=1}^l \frac{1}{2\mu_{h^{(i)}}} \left\| \mathbf{z}_q^{(i)} - \mathbf{h}_q^{(i)} \right\|^2 + \sum_{j=1}^{l+1} \frac{1}{2\mu_{v^{(j)}}} \left\| \mathbf{W}^{(j)} \right\|_F^2}_{\text{I}} \\ + \underbrace{\sum_{q=1}^n \sum_{i=1}^l \alpha_i \left\| \mathbf{h}_q^{(i)} \right\|_1 + \sum_{j=1}^{l+1} \beta_j \left\| \mathbf{V}^{(j)} \right\|_* + r_{\theta}(\boldsymbol{\theta})}_{\text{II}}. \end{aligned} \quad (31)$$

Part I of the objective is smooth and can be written as

$$\begin{aligned} g(\mathbf{h}_{1:n}^{(1:l)}, \mathbf{V}^{(1:l+1)}, \boldsymbol{\theta}) = \mathcal{L}(\boldsymbol{\theta}) + \sum_{q=1}^n \sum_{i=1}^l \frac{1}{2\mu_{h^{(i)}}} \left\| \mathbf{z}_q^{(i)} - \mathbf{h}_q^{(i)} \right\|^2 \\ + \sum_{j=1}^{l+1} \frac{1}{2\mu_{v^{(j)}}} \left\| \mathbf{W}^{(j)} - \mathbf{V}^{(j)} \right\|_F^2, \end{aligned} \quad (32)$$

where $\mathbf{h}_{1:n}^{(1:l)} = \{\mathbf{h}_1^{(1)}, \dots, \mathbf{h}_1^{(l)}, \dots, \mathbf{h}_n^{(1)}, \dots, \mathbf{h}_n^{(l)}\}$ and $\mathbf{V}^{(1:l+1)} = \{\mathbf{V}^{(1)}, \dots, \mathbf{V}^{(l+1)}\}$, respectively. We also employ the following definitions for part II

$$\begin{aligned} r_h(\mathbf{h}_q^{(i)}) = \alpha_i \left\| \mathbf{h}_q^{(i)} \right\|_1, \quad q = 1, \dots, n; i = 1, \dots, l, \\ r_v(\mathbf{V}^{(j)}) = \beta_j \left\| \mathbf{V}^{(j)} \right\|_*, \quad j = 1, \dots, l+1. \end{aligned} \quad (33)$$

Now, we define the optimization problem

$$\begin{aligned} \mathcal{P}_{\mu} : \arg \min_{\mathcal{X}} Q(\mathbf{h}_{1:n}^{(1:l)}, \mathbf{V}^{(1:l+1)}, \boldsymbol{\theta}) = g(\mathbf{h}_{1:n}^{(1:l)}, \mathbf{V}^{(1:l+1)}, \boldsymbol{\theta}) \\ + \sum_{q=1}^n \sum_{i=1}^l r_h(\mathbf{h}_q^{(i)}) + \sum_{j=1}^{l+1} r_v(\mathbf{V}^{(j)}) + r_{\theta}(\boldsymbol{\theta}). \end{aligned} \quad (34)$$

In order to deal with \mathcal{P}_μ , we propose an alternating minimization method by updating all variables $\{\mathbf{h}_q^{(i)}\}_{q=1}^n|_{i=1}^l$, $\{\mathbf{V}^{(j)}\}_{j=1}^{l+1}$, and $\boldsymbol{\theta}$, where at each iteration (epoch) we minimize a second-order upper bound of the objective function. In order to update the parameters of the DNN, $\boldsymbol{\theta}$, we need to construct the loss function presented in (34) in each epoch by passing all training data through the DNN once. Before any training data is entered into the DNN, $\boldsymbol{\theta}_0 = [\text{vec}(\mathbf{W}_0^{(1)}), \dots, \text{vec}(\mathbf{W}_0^{(l+1)}), \mathbf{b}_0^{(1)}, \dots, \mathbf{b}_0^{(l+1)}]$ initializes the parameters of the DNN.

Assuming being in the k -th epoch, the training data 1 to n are entered into the DNN and $\mathbf{h}_{1,k}^{(1)}, \dots, \mathbf{h}_{1,k}^{(l)}, \dots, \mathbf{h}_{n,k}^{(1)}, \dots, \mathbf{h}_{n,k}^{(l)}, \mathbf{V}^{(1)}, \dots, \mathbf{V}^{(l)}$ are calculated, and $\boldsymbol{\theta}_k$ is updated. The general update for $\mathbf{h}_q^{(i)}, \mathbf{V}^{(j)}$ and $\boldsymbol{\theta}$ after the k -th epoch are as follows

$$\mathbf{h}_{q,k}^{(i)} = \arg \min_{\mathbf{h}_q^{(i)}} g(\mathbf{h}_{1:q-1,k}^{(1:l)}, \mathbf{h}_{q,k}^{(<i)}, \mathbf{h}_q^{(i)}, \mathbf{h}_{q,k-1}^{(>i)}, \mathbf{h}_{q+1:n,k-1}^{(1:l)}, \mathbf{V}_{k-1}^{(1:l+1)}, \boldsymbol{\theta}_{k-1}) + r_h(\mathbf{h}_q^{(i)}), \quad k = 1, \dots, K, \quad (35a)$$

$$\mathbf{V}_k^{(j)} = \arg \min_{\mathbf{V}_k^{(j)}} g(\mathbf{h}_{1:n,k}^{(1:l)}, \mathbf{V}_k^{(<j)}, \mathbf{V}^{(j)}, \mathbf{V}_{k-1}^{(>j)}, \boldsymbol{\theta}_{k-1}) + r_v(\mathbf{V}_k^{(j)}), \quad k = 1, \dots, K, \quad (35b)$$

$$\boldsymbol{\theta}_k = \arg \min_{\boldsymbol{\theta}} g(\mathbf{h}_{1:n,k}^{(1:l)}, \mathbf{V}_k^{(1:l+1)}, \boldsymbol{\theta}) + r_\theta(\boldsymbol{\theta}), \quad k = 1, \dots, K. \quad (35c)$$

We consider the order of optimization as $\boldsymbol{\theta}_0$ (initialization), $\mathbf{h}_{1,1}^{(1)} \rightarrow \dots \rightarrow \mathbf{h}_{1,1}^{(l)} \rightarrow \dots \rightarrow \mathbf{h}_{n,1}^{(1)} \rightarrow \dots \rightarrow \mathbf{h}_{n,1}^{(l)} \rightarrow \mathbf{V}_1^{(1)} \rightarrow \dots \rightarrow \mathbf{V}_1^{(l+1)} \rightarrow \boldsymbol{\theta}_1 \rightarrow \mathbf{h}_{1,2}^{(1)} \rightarrow \dots \rightarrow \mathbf{h}_{1,2}^{(l)} \rightarrow \dots \rightarrow \mathbf{h}_{n,2}^{(1)} \rightarrow \mathbf{h}_{n,2}^{(l)} \rightarrow \mathbf{V}_2^{(1)} \rightarrow \dots \rightarrow \mathbf{V}_2^{(l+1)} \rightarrow \boldsymbol{\theta}_2 \rightarrow \mathbf{h}_{1,K}^{(1)} \rightarrow \dots \rightarrow \mathbf{h}_{1,K}^{(l)} \rightarrow \dots \rightarrow \mathbf{h}_{n,K}^{(1)} \rightarrow \dots \rightarrow \mathbf{h}_{n,K}^{(l)} \rightarrow \mathbf{V}_K^{(1)} \rightarrow \dots \rightarrow \mathbf{V}_K^{(l+1)} \rightarrow \boldsymbol{\theta}_K$.

Problems (35a), (35b), and (35c) are nonsmooth, and we follow the same procedure as in [50] to provide closed-form solutions for the updates. We write the derivation for $\boldsymbol{\theta}$. Let us approximate the objective with a quadratic form around $\boldsymbol{\theta}_{k-1}$, i.e.,

$$\begin{aligned} \hat{g}(\mathbf{h}_{1:n,k}^{(1:l)}, \mathbf{V}_k^{(1:l+1)}, \boldsymbol{\theta}) &= g(\mathbf{h}_{1:n,k}^{(1:l)}, \mathbf{V}_k^{(1:l+1)}, \boldsymbol{\theta}_{k-1}) \\ &+ \nabla_{\boldsymbol{\theta}}^T g(\mathbf{h}_{1:n,k}^{(1:l)}, \mathbf{V}_k^{(1:l+1)}, \boldsymbol{\theta}_{k-1})(\boldsymbol{\theta} - \boldsymbol{\theta}_{k-1}) \\ &+ \frac{1}{2}(\boldsymbol{\theta} - \boldsymbol{\theta}_{k-1})^T \mathbf{H}_\theta(\mathbf{h}_{1:n,k}^{(1:l)}, \mathbf{V}_k^{(1:l+1)}, \boldsymbol{\theta}_{k-1})(\boldsymbol{\theta} - \boldsymbol{\theta}_{k-1}), \end{aligned} \quad (36)$$

where $\nabla_{\boldsymbol{\theta}}^T g(\cdot)$ and $\mathbf{H}_\theta(\cdot)$ stand for gradient and Hessian of $g(\mathbf{h}_{1:n,k}^{(1:l)}, \mathbf{V}_k^{(1:l+1)}, \boldsymbol{\theta}_{k-1})$ with respect to $\boldsymbol{\theta}$ with $\mathbf{h}_{1:n}^{(1:l)} = \mathbf{h}_{1:n,k}^{(1:l)}, \mathbf{V}^{(1:l+1)} = \mathbf{V}_k^{(1:l+1)}$. In Proposition 1, we will show that the gradient of $g(\mathbf{h}_{1:n}^{(1:l)}, \mathbf{V}^{(1:l+1)}, \boldsymbol{\theta})$ is Lipschitz, and an upper bound for the second-order approximation as

$$\begin{aligned} \hat{g}(\mathbf{h}_{1:n,k}^{(1:l)}, \mathbf{V}_k^{(1:l+1)}, \boldsymbol{\theta}) &\leq g(\mathbf{h}_{1:n,k}^{(1:l)}, \mathbf{V}_k^{(1:l+1)}, \boldsymbol{\theta}_{k-1}) \\ &+ \nabla_{\boldsymbol{\theta}}^T g(\mathbf{h}_{1:n,k}^{(1:l)}, \mathbf{V}_k^{(1:l+1)}, \boldsymbol{\theta}_{k-1})(\boldsymbol{\theta} - \boldsymbol{\theta}_{k-1}) \\ &+ \frac{1}{2\mu_{\theta,k}} \|\boldsymbol{\theta} - \boldsymbol{\theta}_{k-1}\|^2 =: \tilde{g}(\mathbf{h}_{1:n,k}^{(1:l)}, \mathbf{V}_k^{(1:l+1)}, \boldsymbol{\theta}), \end{aligned} \quad (37)$$

for $\mu_{\theta,k} \in (0, \frac{1}{L_{\theta,k}}]$. Using (37) in (35c), we have

$$\begin{aligned} \boldsymbol{\theta}_k &= \arg \min_{\boldsymbol{\theta}} g(\mathbf{h}_{1:n,k}^{(1:l)}, \mathbf{V}_k^{(1:l+1)}, \boldsymbol{\theta}_{k-1}) + \nabla_{\boldsymbol{\theta}}^T g(\mathbf{h}_{1:n,k}^{(1:l)}, \mathbf{V}_k^{(1:l+1)}, \boldsymbol{\theta}_{k-1})(\boldsymbol{\theta} - \boldsymbol{\theta}_{k-1}) \\ &+ \frac{1}{2\mu_{\theta,k}} \|\boldsymbol{\theta} - \boldsymbol{\theta}_{k-1}\|^2 + r_\theta(\boldsymbol{\theta}). \end{aligned} \quad (38)$$

Since the convergence rate of the proximal gradient algorithm is slow, it has been suggested to use the extrapolated version of the last two estimates to update the next one [51]. Hence, we suggest the extrapolated version as

$$\begin{aligned} \boldsymbol{\theta}_k &= \arg \min_{\boldsymbol{\theta}} g(\mathbf{h}_{1:n,k}^{(1:l)}, \mathbf{V}_k^{(1:l+1)}, \hat{\boldsymbol{\theta}}_{k-1}) + \nabla_{\boldsymbol{\theta}}^T g(\mathbf{h}_{1:n,k}^{(1:l)}, \mathbf{V}_k^{(1:l+1)}, \hat{\boldsymbol{\theta}}_{k-1})(\boldsymbol{\theta} - \hat{\boldsymbol{\theta}}_{k-1}) \\ &+ \frac{1}{2\mu_{\theta,k}} \|\boldsymbol{\theta} - \hat{\boldsymbol{\theta}}_{k-1}\|^2 + r_\theta(\boldsymbol{\theta}), \end{aligned} \quad (39)$$

in which $\hat{\boldsymbol{\theta}}_{k-1}$ is defined by

$$\hat{\boldsymbol{\theta}}_{k-1} = \boldsymbol{\theta}_{k-1} + \omega_{\theta,k}(\boldsymbol{\theta}_{k-1} - \boldsymbol{\theta}_{k-2}), \quad (40)$$

where $\omega_{\theta,k} > 0$ is the extrapolation weight. Simple manipulations of (39) lead to

$$\begin{aligned} \boldsymbol{\theta}_k &= \arg \min_{\boldsymbol{\theta}} \frac{1}{2\mu_{\theta,k}} \\ &\times \left\| \boldsymbol{\theta} - \left(\hat{\boldsymbol{\theta}}_{k-1} - \mu_{\theta,k} \nabla_{\boldsymbol{\theta}} g(\mathbf{h}_{1:n,k}^{(1:l)}, \mathbf{V}_k^{(1:l+1)}, \hat{\boldsymbol{\theta}}_{k-1}) \right) \right\|^2 + r_\theta(\boldsymbol{\theta}). \end{aligned} \quad (41)$$

which is equivalent to the proximal iteration

$$\boldsymbol{\theta}_k = \text{Prox}_{\mu_{\theta,k}, r_\theta} \left(\hat{\boldsymbol{\theta}}_{k-1} - \mu_{\theta,k} \nabla_{\boldsymbol{\theta}} g(\mathbf{h}_{1:n,k}^{(1:l)}, \mathbf{V}_k^{(1:l+1)}, \hat{\boldsymbol{\theta}}_{k-1}) \right). \quad (42)$$

The same procedure can be written for $\mathbf{h}_{q,k}^{(i)}$ and $\mathbf{V}_k^{(j)}$

$$\begin{aligned} \mathbf{h}_{q,k}^{(i)} &= \text{Prox}_{\mu_{h^{(i)},k}, \alpha_i \|\mathbf{h}_q^{(i)}\|_1} \left(\mathbf{h}_{q,k-1}^{(i)} - \mu_{h^{(i)},k} \nabla_{\mathbf{h}_q^{(i)}} g(\mathbf{h}_{1:q-1,k}^{(1:l)}, \mathbf{h}_{q,k}^{(<i)}, \mathbf{h}_{q,k-1}^{(i)}, \mathbf{h}_{q,k-1}^{(>i)}, \mathbf{h}_{q+1:n,k-1}^{(1:l)}, \mathbf{V}_{k-1}^{(1:l+1)}, \boldsymbol{\theta}_{k-1}) \right) \\ &= \text{Prox}_{\mu_{h^{(i)},k}, \alpha_i \|\mathbf{h}_q^{(i)}\|_1} \left(\mathbf{z}_{q,k-1}^{(i)} \right), \quad k = 1, \dots, K. \end{aligned} \quad (43)$$

where

$$\mathbf{z}_{q,k-1}^{(i)} = g^{(i)} \left(\mathbf{W}_{k-2}^{(i)} \left(\dots \left(g^{(1)}(\mathbf{W}_{k-2}^{(1)} \mathbf{x}_q + \mathbf{b}_{k-2}^{(1)}) \right) \dots \right) + \mathbf{b}_{k-2}^{(i)} \right). \quad (44)$$

We write (43) for $k=1,2$

$$\begin{aligned} \mathbf{h}_{q,1}^{(i)} &= \text{Prox}_{\mu_{h^{(i)},k}, \alpha_i \|\mathbf{h}_q^{(i)}\|_1} \left(\mathbf{z}_{q,0}^{(i)} \right), \\ \mathbf{h}_{q,2}^{(i)} &= \text{Prox}_{\mu_{h^{(i)},k}, \alpha_i \|\mathbf{h}_q^{(i)}\|_1} \left(\mathbf{z}_{q,1}^{(i)} \right). \end{aligned} \quad (45)$$

In (45), we need $\boldsymbol{\theta}_{-1}$ and $\boldsymbol{\theta}_0$ to calculate $\mathbf{z}_{q,0}$ and $\mathbf{z}_{q,1}$. We initialize $\boldsymbol{\theta}_0$ randomly and set $\boldsymbol{\theta}_{-1} = \boldsymbol{\theta}_0$.

In the same way, we obtain

$$\begin{aligned} \mathbf{V}_k^{(j)} &= \text{Prox}_{\mu_{v^{(j)},k}, \beta_j \|\mathbf{V}^{(j)}\|_*} \left(\mathbf{V}_{k-1}^{(j)} - \mu_{v^{(j)},k} \right. \\ &\quad \left. \nabla_{v^{(j)}} g \left(\mathbf{h}_{1:n,k}^{(1:l)}, \mathbf{V}_k^{(<i)}, \mathbf{V}_{k-1}^{(j)}, \mathbf{V}_{k-1}^{(>i)}, \boldsymbol{\theta}_{k-1} \right) \right) \quad (46) \\ &= \text{Prox}_{\mu_{v^{(j)},k}, \beta_j \|\mathbf{V}^{(j)}\|_*} \left(\mathbf{W}_{k-1}^{(j)} \right). \end{aligned}$$

Alternative updates of the above-mentioned parameters lead to the following algorithm for training the FCNNs in which we aim at computing the missing entries of the partially observed matrix satisfying

$$x_{ij} = \hat{x}_{ij}, \quad (i, j) \in \bar{\Omega}, \quad (47)$$

where $\bar{\Omega}$ shows the missing entries.

A. Convergence Analysis

Employing smooth enough activation functions in a DNN, most of the times, the loss function defined for training this network will be nonconvex. Without assuming the convexity of the loss function and by bounding the parameters of the network by adding the regularization terms $r_\theta(\boldsymbol{\theta})$, we show that the sequence generated by the DNN-NSR algorithm converges to the critical point of the \mathcal{P}_μ .

Proposition 1. *Partial derivatives of function $g(\mathbf{h}_{1:n}^{(1:l)}, \mathbf{V}^{(1:l+1)}, \boldsymbol{\theta})$ (defined in (32)) with respect to $\mathbf{h}_q^{(i)}$ and $\mathbf{V}^{(j)}$ are Lipschitz continuous. Moreover, if all activation functions $g^{(i)}$ ($i \in \{1, \dots, l\}$) used in (15) are twice continuously differentiable and $\mathcal{C} = \{\boldsymbol{\theta} \in \mathbb{R}^d \mid \|\boldsymbol{\theta}\|_\infty \leq M\}$, then the partial derivative of $g(\mathbf{h}_{1:n}^{(1:l)}, \mathbf{V}^{(1:l+1)}, \boldsymbol{\theta})$ with respect to $\boldsymbol{\theta}$ is Lipschitz continuous on \mathcal{C} .*

Proof. See Appendix A. \square

Let us emphasize that introducing the compact set \mathcal{C} in Proposition 1 is essential to show that partial derivative of $g(\mathbf{h}_{1:n}^{(1:l)}, \mathbf{V}^{(1:l+1)}, \boldsymbol{\theta})$ with respect to $\boldsymbol{\theta}$ is L -Lipschitz continuous. Indeed, this partial derivative is not Lipschitz continuous on \mathbb{R}^d . For example, if we assume the simplest case that all activation functions are identity, then it is shown in [52] that the resulting loss function is relatively smooth in the sense discussed in [53], [54], and non-Euclidean proximal operators in the sense of Bregman distances. The way to remove this constraint involves much more technical details, multi-block relative smoothness in the sense defined in [55], [56], [57], which is out of the scope of the current paper that we postpone to future studies. Invoking Proposition 1, a step-size can be obtained for each optimization variable, for which it is guaranteed that the value of the objective function decreases. Note that step-sizes depend on these Lipschitz constants.

Proposition 2. *Let all assumptions of Proposition 1 be satisfied, and let $\{\{\mathbf{h}_{q,k}^{(i)}\}_{q=1}^n\}_{i=1}^l, \{\mathbf{V}_k^{(j)}\}_{j=1}^{l+1}, \boldsymbol{\theta}_k\}$ be the sequence generated by the update rules introduced in (43), (46), and (42), respectively. Then, it holds that*

$$\begin{aligned} &\sum_{k=1}^{\infty} \sum_{q=1}^n \sum_{i=1}^l \nu_{h^{(i)},k} \|\mathbf{h}_{q,k}^{(i)} - \mathbf{h}_{q,k-1}^{(i)}\|^2 + \sum_{k=1}^{\infty} \sum_{j=1}^{l+1} \nu_{v^{(j)},k} \|\mathbf{V}_k^{(j)} \\ &\quad - \mathbf{V}_{k-1}^{(j)}\|_F^2 + \sum_{k=1}^{\infty} \nu_{\theta,k} \|\boldsymbol{\theta}_k - \boldsymbol{\theta}_{k-1}\|^2 < \infty, \quad (48) \end{aligned}$$

Algorithm 1 Deep Neural Network with Nonsmooth Regularization terms (DNN-NSR) to solve NLMC problem.

1: **Input:** Ω , \mathbf{X} , M in (8), $\{\alpha_i\}_{i=1}^l$, $\{\beta_j\}_{j=1}^{l+1}$, number of epochs K , n is the number of columns of \mathbf{X} , λ in (21), $\mu_{h^{(i)}}^{\max}$, $\mu_{h^{(i)}}^{\min}$, $\mu_{v^{(i)}}^{\max}$, $\mu_{v^{(i)}}^{\min}$, μ_θ^{\max} , μ_θ^{\min} , $\gamma = 10^3$, $s_1 = \{0.1, 0.2, 0.8, 0.9\}$ (scale value for all μ), $s_2 = \{0.1, 0.2, 0.5, 0.6\}$, $s_3 = \{1.05, 1.1, 1.2\}$, termination threshold $(\{\zeta_i\}_{i=1}^l, \{\zeta_j\}_{j=1}^{l+1})$, E is a specific epoch number (e.g. $E = 200, 300$), $\delta_{\min} = 0.01$, $\delta_1 = \delta_{\max} = 0.99$.
2: **Initialization:** $\boldsymbol{\theta}_0 = \boldsymbol{\theta}_{-1}$.
3: **Output:** x_{ij} in (47), Neural Network parameters.

4: $\mu^{\max} = \mu_{h^{(i)}}^{\max}, \mu_{v^{(j)}}^{\max}, \mu_\theta^{\max}$
5: **for** $k = 1, 2, \dots, K$ **do**
6: $\mu_{\theta,k} = \frac{1}{\gamma L_{\theta,k}}$, $\mu_{\theta,0} = \mu_{\theta,1} = \mu_\theta^{\max}$;
7: $\omega_{\theta,1} = \frac{\gamma-1}{2(\gamma+1)} \sqrt{\delta_1} \approx 0.5$, $k = 1$;
8: $\omega_{\theta,k} = \frac{\gamma-1}{2(\gamma+1)} \sqrt{\delta_k \frac{L_{\theta,k-1}}{\mu_{L,k}}} \approx 0.5 \sqrt{\delta_k \frac{L_{\theta,k-1}}{\mu_{L,k}}}$, $k \geq 2$;
9: **if** equation (3) in the supplementary materials is not satisfied **then**
10: $\mu^{\max} \leftarrow s_1 \cdot \mu^{\max}$;
11: **else**
12: **for** $q = 1, 2, \dots, n$ **do**
13: Compute $\{\mathbf{h}_{q,k}^{(i)}\}_{i=1}^l$ using (43) ;
14: **end for**
15: Compute $\{\mathbf{V}_k^{(j)}\}_{j=1}^{l+1}$ using (46) ;
16: $\hat{\boldsymbol{\theta}}_{k-1} = \boldsymbol{\theta}_{k-1} + \omega_{\theta,k} (\boldsymbol{\theta}_{k-1} - \boldsymbol{\theta}_{k-2})$;
17: Compute $\boldsymbol{\theta}_k$ using (42) ;
18: Calculate $Q(\xi_k) = Q(\mathbf{h}_{1:n,k}^{(1:l)}, \mathbf{V}_k^{(1:l+1)}, \boldsymbol{\theta}_k)$ using (34);
19: Calculate $Q(\xi_{k-1}) = Q(\mathbf{h}_{1:n,k-1}^{(1:l)}, \mathbf{V}_{k-1}^{(1:l+1)}, \boldsymbol{\theta}_{k-1})$ using (34);
20: **if** $Q(\xi_k) - Q(\xi_{k-1}) > 0$ ($k > E$) **then**
21: $\delta_k = s_2 \cdot \delta_{k-1}$;
22: **if** $\delta_k < \delta_{\min}$ **then**
23: $\delta_k \leftarrow \delta_{\min}$;
24: **end if**
25: Repeat lines 4 to 26 with new μ^{\max} .
26: **end if**
27: **if** $Q(\xi_k) - Q(\xi_{k-1}) < 0$ ($k > E$) **then**
28: $\delta_k = s_3 \cdot \delta_{k-1}$;
29: **if** $\delta_k > \delta_{\max}$ **then**
30: $\delta_k \leftarrow \delta_{\max}$;
31: **end if**
32: Calculate $C1_k = \|\mathbf{h}_{1:n,k}^{(i)} - \mathbf{z}_{1:n,k}^{(i)}\|^2 \leq \zeta_i$;
33: Calculate $C2_k = \|\mathbf{V}_k^{(j)} - \mathbf{W}_k^{(j)}\|^2 \leq \zeta_j$;
34: **if** $k = K$ or $C1_k$ and $C2_k$ satisfied **then**
35: calculate x_{ij} according to (47);
36: **else**
37: continue until $k = K$ or satisfy $C1_k$ and $C2_k$;
38: **end if**
39: **end if**
40: **end if**
41: **end for**

with $\nu_{h^{(i)},k} = \frac{(\gamma-1)L_{h^{(i)},k}}{2}$, $\nu_{v^{(j)},k} = \frac{(\gamma-1)L_{v^{(j)},k}}{2}$, $\nu_{\theta,k} = \frac{(1-\delta_{k+1})(\gamma-1)L_{\theta,k}}{2}$, and $\omega_{\theta,k} \leq \frac{\gamma-1}{2(\gamma+1)}\sqrt{\delta_k \frac{L_{\theta,k-1}}{L_{\theta,k}}}$ for $\delta_k < 1$ and $\gamma > 1$.

Proof. See Appendix B. \square

Proposition 3. *If the function Q given in (34) has bounded lower level sets, then $\{\{\mathbf{h}_k^{(i)}\}_{i=1}^l, \{\mathbf{V}_k^{(j)}\}_{j=1}^{l+1}, \boldsymbol{\theta}_k\}$ generated by Algorithm 1 is a bounded sequence.*

Proof. See Appendix C. \square

Theorem 1 (Subsequence convergence:). *Let $\{\{\mathbf{h}_k^{(i)}\}_{i=1}^l, \{\mathbf{V}_k^{(j)}\}_{j=1}^{l+1}, \boldsymbol{\theta}_k\}$ be a bounded sequence generated by Algorithm 1, then*

- (a) *There exists a finite limit point (say $\{\{\bar{\mathbf{h}}^{(i)}\}_{i=1}^l, \{\bar{\mathbf{V}}^{(j)}\}_{j=1}^{l+1}, \bar{\boldsymbol{\theta}}\}$) for the sequence.*
 (b) *Regularizers satisfy:*

$$\begin{aligned} \lim_{\mathcal{I} \ni k \rightarrow \infty} r_h(\mathbf{h}_k^{(i)}) &= r_h(\bar{\mathbf{h}}^{(i)}), \quad i = 1, \dots, l, \\ \lim_{\mathcal{I} \ni k \rightarrow \infty} r_v(\mathbf{V}_k^{(j)}) &= r_v(\bar{\mathbf{V}}^{(j)}), \quad j = 1, \dots, l+1, \\ \lim_{\mathcal{I} \ni k \rightarrow \infty} r_\theta(\boldsymbol{\theta}) &= r_\theta(\bar{\boldsymbol{\theta}}), \end{aligned} \quad (49)$$

where \mathcal{I} stands for the subsequence index set.

- (c) *Any limit point of the sequence is a critical point of the function $Q(\mathbf{h}^{(1:l)}, \mathbf{V}^{(1:l+1)}, \boldsymbol{\theta})$ in (34).*
 (d) *If a subsequence $\{\{\mathbf{h}_k^{(i)}\}_{i=1}^l, \{\mathbf{V}_k^{(j)}\}_{j=1}^{l+1}, \boldsymbol{\theta}_k\}_{k \in \mathcal{I}}$ converges to $\{\{\bar{\mathbf{h}}^{(i)}\}_{i=1}^l, \{\bar{\mathbf{V}}^{(j)}\}_{j=1}^{l+1}, \bar{\boldsymbol{\theta}}\}$, then we have*

$$\lim_{\mathcal{I} \ni k \rightarrow \infty} Q(\mathbf{h}_k^{(1:l)}, \mathbf{V}_k^{(1:l+1)}, \boldsymbol{\theta}_k) = Q(\bar{\mathbf{h}}^{(1:l)}, \bar{\mathbf{V}}^{(1:l+1)}, \bar{\boldsymbol{\theta}}). \quad (50)$$

Proof. See Appendix D. \square

Based on Theorem 1, there exists a subsequence in the sequence generated by Algorithm 1 that converges to the critical point of Q . In order to prove the convergence of the whole sequence, we further assume that function Q satisfies the KL property.

Proposition 4. *The objective function $Q(\mathbf{h}^{(1:l)}, \mathbf{V}^{(1:l+1)}, \boldsymbol{\theta})$, defined in (34), is a KL function.*

Proof. As stated in (34), $Q(\mathbf{h}_k^{(1:l)}, \mathbf{V}_k^{(1:l+1)}, \boldsymbol{\theta}_k)$ contains different terms. In [38], it has been shown that $g(\mathbf{h}_k^{(1:l)}, \mathbf{V}_k^{(1:l+1)}, \boldsymbol{\theta}_k)$ and $r_\theta(\boldsymbol{\theta})$ have the KL property. The KL property for the ℓ_1 norm and the nuclear norm was studied in [58]. Therefore, Q possesses the KL property. \square

To show the whole sequence convergence, we borrow Theorem 2.7 from [50], which will be presented in the next result.

Theorem 2 (Global convergence [50]:). *Consider problem (34) where $Q(\mathbf{h}^{(1:l)}, \mathbf{V}^{(1:l+1)}, \boldsymbol{\theta})$ is proper and bounded in $\text{dom}(F)$, $g(\mathbf{h}^{(1:l)}, \mathbf{V}^{(1:l+1)}, \boldsymbol{\theta})$ is continuously differentiable, $\{r_h(\mathbf{h}^{(i)})\}_{i=1}^l$, $\{r_v(\mathbf{V}^{(j)})\}_{j=1}^{l+1}$ and $r_\theta(\boldsymbol{\theta})$ are proper and l.s.c., $g(\mathbf{h}^{(1:l)}, \mathbf{V}^{(1:l+1)}, \boldsymbol{\theta})$ has Lipschitz gradient with respect to all variables and the problem has a critical point \mathbf{x}^* , where*

$\mathbf{0} \in \partial F(\mathbf{x}^*)$. *Let $\{\mathbf{h}^{(1:l)}(k), \mathbf{V}^{(1:l+1)}(k), \boldsymbol{\theta}(k)\}_{k \geq 1}$ be generated from Algorithm 1. Assume:*

- (a) $\{\mathbf{h}_k^{(1:l)}, \mathbf{V}_k^{(1:l+1)}, \boldsymbol{\theta}_k\}_{k \geq 1}$ has a finite limit point $\{\bar{\mathbf{h}}^{(1:l)}, \bar{\mathbf{V}}^{(1:l+1)}, \bar{\boldsymbol{\theta}}\}$.
 (b) *If $Q(\mathbf{h}^{(1:l)}, \mathbf{V}^{(1:l+1)}, \boldsymbol{\theta})$ is a KL function, then*

$$\lim_{k \rightarrow \infty} \{\mathbf{h}_k^{(1:l)}, \mathbf{V}_k^{(1:l+1)}, \boldsymbol{\theta}_k\} = \{\bar{\mathbf{h}}^{(1:l)}, \bar{\mathbf{V}}^{(1:l+1)}, \bar{\boldsymbol{\theta}}\}. \quad (51)$$

Using Theorem 2, we can easily show that the sequence generated by Algorithm 1 converges to a critical point of the problem \mathcal{P}_μ .

Theorem 3. *The sequence $\{\mathbf{h}_k^{(1:l)}, \mathbf{V}_k^{(1:l+1)}, \boldsymbol{\theta}_k\}_{k \geq 1}$ generated by Algorithm 1 converges to a critical point of problem $\mathcal{P}_{\mu_i, \mu_j}$ defined in (34).*

Proof. See [38, Theorem 3]. \square

V. EXPERIMENTAL RESULTS

In this section, a series of experiments on both synthetic and real data are conducted to evaluate the performance of the proposed matrix completion algorithm. We compare the results of the proposed algorithm with five algorithms, IALM [15], NCARL [23], AEMC [33], DLMC [33], and BiBNN [36]. The first two algorithms are of LRMC type, while the others are based on DNNs and NLMC. In all simulations, we set $\alpha_i = \beta_j = 0.1$ in (27) and $\lambda = 10^{-3}$ in (19). The optimal value of the extrapolation weight, $\omega_{\theta,k}$, is different for various experiments and missing rates, so we set its optimal value for each experiment using search in $[0, \omega_{\theta,k} \approx 0.5\sqrt{\delta_k \frac{L_{\theta,k-1}}{L_{\theta,k}}}]$ interval with step-size 0.05, and the value with the highest convergence rate is chosen as the optimal value of $\omega_{\theta,k}$. We choose a significant value for $\mu = \mu_{max}$ at the beginning epochs of training whether to satisfy (3) (descent lemma) (please see the equation (3) in supplementary materials) and gradually reduce it using a cosine annealing schedule to $\mu = \mu_{min}$ to increase the effect of the regularization terms. We have chosen $\mu_{min} = 1$ in all experiments, but μ_{max} is sensitive to the missing rate and datasets and is determined accordingly. If the hyperparameter values differ from those mentioned earlier, it will be stated in the experiment.

A. Synthetic Matrix Completion

To evaluate the performance of the proposed method, we generate a synthetic data with an $m \times n$ matrix of rank r as follows:

$$\mathbf{X} = g \left(1.2 \left(0.5g^2(\mathbf{A}\mathbf{B}) - g(\mathbf{A}\mathbf{B}) - 1 \right) \right) + \mathbf{A}\mathbf{B}, \quad (52)$$

where $\mathbf{A} \in \mathbb{R}^{m \times r}$ and $\mathbf{B} \in \mathbb{R}^{r \times n}$. Both matrices have independent and identically distributed (i.i.d.) standard Gaussian entries. $g(x) = 1.71 \tanh(\frac{2}{3}x)$ is an element-wise activation function as in [33]. We use (52) to make $\mathbf{X} \in \mathbb{R}^{300 \times 200}$ matrices, $r = 10$. Then randomly remove 10%, 30%, 50%, and 80% of the entries.

TABLE I: PSNRs, SDs, and MSEs on synthetic matrix $\mathbf{X} \in \mathbb{R}^{300 \times 200}$ with $\rho = 10\%, 30\%, 50\%$, and 80% .

$\rho(\%)$	Metric	IALM	NCARL	AEMC	DLMC	BiBNN	DNN-NSR
10	PSNR	26.1469	30.3217	30.5333	32.5475	35.2654	37.3565
	SD	0.6883	0.6617	0.6655	0.6592	0.7553	0.5672
	MSE	15.4390	4.8132	4.5421	3.7843	3.2200	1.9130
30	PSNR	20.5052	24.4008	24.0187	27.4959	32.9584	35.1072
	SD	0.8169	0.6915	0.6056	0.7185	0.7552	0.6594
	MSE	18.2639	6.8739	6.4113	4.3082	3.4340	2.7940
50	PSNR	17.8976	21.5373	18.1350	25.7063	27.1325	29.8678
	SD	0.9126	0.9723	0.6433	0.6414	0.6370	0.6749
	MSE	22.7209	14.3484	12.2660	10.0870	8.3160	4.1823
80	PSNR	12.3161	17.7434	17.6322	20.6940	21.2342	25.0967
	SD	0.5247	0.4662	0.6706	0.4890	0.5081	0.3929
	MSE	48.8798	27.1525	27.9435	24.9295	24.4341	18.5580

The peak signal-to-noise ratio (PSNR) [59] is employed to evaluate the performance of the proposed method for synthetic matrix and image inpainting, defined as:

$$\text{PSNR} = 10 \log_{10} \frac{mn(\max(\mathbf{X}))^2}{\|\hat{\mathbf{X}} - \mathbf{X}\|_F^2}, \quad (53)$$

where \mathbf{X} and $\hat{\mathbf{X}}$ are the observed and the recovered matrices, respectively, and $\max(\mathbf{X})$ is the maximum element in \mathbf{X} . The following MSE is used to evaluate the performance of matrix completion [33]:

$$\text{MSE} = \frac{\sum_{i,j \in \bar{\Omega}} (\hat{x}_{ij} - x_{ij})^2}{\sum_{i,j \in \bar{\Omega}} x_{ij}^2}. \quad (54)$$

Larger PSNR and smaller MSE reflect better recovery results. In this experiment, the PSNRs and MSEs presented in Table I represents the mean values obtained from ten repeated trials each for LRMC and for training DNNs from scratch. We use a partially observed matrix to train the neural network. The stability of the proposed method is measured by the standard deviation (SD) of PSNRs.

In the synthesis matrices, $\mu_{\max} = 10^5$ for the missing rate, $\rho = 80\%$, and 10^6 for the rest of the missing rates.

MSE is an excellent criterion to monitor over-fitting because it only performs calculations based on unobserved entries. The results reported in Table I shows that the DNN-NSR algorithm performs better than the other five. The PSNR criterion improvement for \mathbf{X} , for $\rho = 10\%$ compared to the best performing BiBNN algorithm, is approximately 2.1 dB, while for $\rho = 80\%$, it is roughly 3.86 dB.

MSE comparisons are also listed in Table I. The highest improvement for the $\mathbf{X} \in \mathbb{R}^{300 \times 200}$ is 5.87 for $\rho = 80\%$. The lowest improvement is for $\rho = 30\%$, equal to 0.64.

Controlling the over-fitting is the main reason for improving the results of the presented algorithm compared to BiBNN, DLMC, and AEMC algorithms. The nonlinearity of the matrix completion model is added for the sake of IALM and NCARL. The low SD value of the DNN-NSR algorithm for most of the missing rates indicates better stability of this algorithm.

B. Single Image Inpainting

One of the applications of matrix completion problems is to recover the missing pixels of an image [16], [59]. The pixel

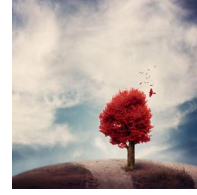


Fig. 1: RGB image for the experiment (Image I) .

values of an RGB image are between 0 and 255, and each pixel is made up of three values red, green, and blue. Each channel of the image is a matrix with the dimensions of the image, and by concatenating the matrix of all three channels, a new matrix is obtained. We consider Image I in Fig.1 and randomly mask their pixels with rates of $\rho = 30\%, 40\%$, and 50% and $\mu_{\max} = 10^6$.

Structure similarity (SSIM) [59] is a measure used to evaluate the quality of the reconstructed image

$$\text{SSIM} = \frac{(2\mu_{\hat{\mathbf{X}}}\mu_{\mathbf{X}} + C_1)(2\sigma_{\hat{\mathbf{X}}\mathbf{X}} + C_2)}{(\mu_{\hat{\mathbf{X}}}^2 + \mu_{\mathbf{X}}^2 + C_1)(\sigma_{\hat{\mathbf{X}}}^2 + \sigma_{\mathbf{X}}^2 + C_2)}, \quad (55)$$

where $\mu_{\hat{\mathbf{X}}}$ and $\mu_{\mathbf{X}}$ are mean values, $\sigma_{\hat{\mathbf{X}}}^2$ and $\sigma_{\mathbf{X}}^2$ are variances, and $\sigma_{\hat{\mathbf{X}}\mathbf{X}}$ is the covariance. $C_1 = 0.01$ and $C_2 = 0.03$ are two constant values that prevent the denominator from becoming zero. A higher value of SSIM represents a better recovery. The SSIM criterion is a number between 0 and 1.

We have used PSNR and SSIM criteria to compare DNN-NSR with five other algorithms. Reported values for both metrics are the average of 10 iterations of the algorithm run. The results of Table II for Image I in Fig. 1 shows that the higher the missing rate of image pixels, the higher the improvement of the presented algorithm with the two mentioned criteria. For example, for a $\rho = 30\%$, we have an improvement of 0.41dB, while this improvement for a $\rho = 50\%$ is 1.1dB. The increase of the SSIM criterion for the missing rates of 30%, 40%, and 50% is 0.0038, 0.0059, and 0.018, respectively.

Fig. 2 represents the result of inpainting for Image I in Fig. 1 when 50% of the pixels are masked, where we can visually inspect the performance.

TABLE II: PSNRs and SSIMs on Image I in Fig. 1 with 30%, 40%, and 50% randomly masked pixels as examples.

$\rho(\%)$	Metric	IALM	NCARL	AEMC	DLMC	BiBNN	DNN-NSR
30	PSNR	16.7313	27.6908	28.4982	29.6249	30.4575	30.8723
	SSIM	0.3434	0.7838	0.8269	0.8629	0.8736	0.8774
40	PSNR	16.7342	26.6660	27.9642	29.3363	29.7862	30.2301
	SSIM	0.3310	0.7606	0.7946	0.8488	0.8597	0.8656
50	PSNR	16.7315	25.9480	27.4329	28.7921	28.9233	30.0301
	SSIM	0.3169	0.7466	0.7221	0.8009	0.8342	0.8521

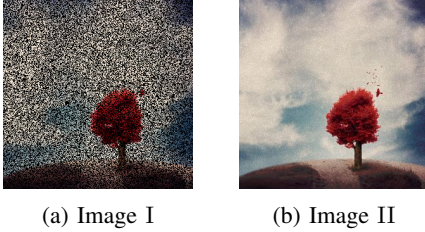


Fig. 2: Masked and inpainted results for Image I in Fig. 1 with 50% random masked pixels, (a): masked image, (b) inpainted image.

C. Recommender System

Another application of matrix completion is recommender systems [11], [12]. Two famous datasets used in recommender systems are MovieLens 100k and MovieLens 1M. In these datasets, users assign scores between 1 and 5 to the movies on the Netflix website. Table III shows some information about the datasets.

A recommender system can be modeled as an incomplete matrix, where the rows and columns of the matrix represent users and films. Thus we have a matrix whose number of available entries is tiny because the number of movies that each user views is small. To train the FCNN, we use 70% and 50% of the available entries for training and the remaining 30% and 50% for testing the DNN-NSR algorithm with $\mu_{\max} = 10^5$.

To measure the performance of the algorithms, we use the Normalized Mean Absolute Error (NMAE) criteria defined as [33]:

$$\text{NMAE} = \frac{1}{(x_{\max} - x_{\min})|\bar{\Omega}|} \sum_{i,j \in \bar{\Omega}} |\hat{x}_{ij} - x_{ij}|, \quad (56)$$

where x_{\max} and x_{\min} are the upper and lower bounds of ratings, respectively, $|\bar{\Omega}|$ is the number of missing entries, and \hat{x}_{ij} and x_{ij} are the actual and recovered ratings of movie j by user i , respectively. The declared NMAE is the average of 10 iterations of the algorithm, and a small NMAE represents better performance.

Table IV shows that the results of the DNN-NSR algorithm are superior. The reason is that the gradual nonsmooth regularization terms have controlled over-fitting.

D. Gradual Learning Effect

The main property of the proposed algorithm is its gradual complexity addition. The following experiment shows how gradual complexity addition helps the training. In this experiment, we set $\mu_{\min} = 1$ and changed the exponent of μ_{\max} from 10^6 to μ_{\min} . We have set the PSNR value for both synthetic data with $\rho = 50\%$ and 80% and Image I in Fig. 1 with random masked pixels $\rho = 40\%$ and 50% . Each number reported in this experiment is the average of over ten runs of the neural network training from scratch.

The result of Table V indicates the effect of gradual complexity addition. Choosing μ_{\max} larger than μ_{\min} leads to better results in all the cases. On the other hand, increasing μ_{\max} will not always work. In the two synthetic data matrices, if ρ increases, we get better performance for smaller μ_{\max} . It originates from the fact that if we have little training data and a considerable value is chosen for μ_{\max} , then μ_{\max} is decreased slowly. Thus the effect of regularization is imposed slowly, which leads to over-fitting. Similar results can be seen for Image I in Fig. 1.

E. Extrapolation Weight Effect

Another important hyper-parameter affecting the proposed algorithm's convergence rate is the extrapolation weight. In this experiment, we inspect this hyper-parameter over the following datasets:

- 1) 300×200 synthetic matrix with $\rho = 80\%$ and $\mu_{\max} = 10^5$.
- 2) Image I in Fig. 1 with 50% random masked pixels and $\mu_{\max} = 10^6$.

Fig. 3 shows the value of loss function versus training epoch for different datasets. Values of $\omega_{\theta,k}$ other than zero generally lead to better performance. This is due to the fact that extrapolated variables carry information from the previous iteration, which can be utilized during the current update. The optimal values for $\omega_{\theta,k}$ in datasets 1, and 2 are 0.45 and $0.5\sqrt{\delta_k \frac{L_{\theta,k-1}}{L_{\theta,k}}}$ in order, where $\omega_{\theta,k} = \sqrt{\delta_k \frac{L_{\theta,k-1}}{L_{\theta,k}}}$ is called **adaptively update**.

VI. CONCLUSION

To solve the NLMC problem, we suggested the DNN-NSR algorithm. Over-fitting control of the neural network is the most critical issue from which the idea of using regularization originated. We have shown that the proximal operator algorithm can be used to train an FCNN with several

TABLE III: Information of MovieLens 100k and 1M.

Dataset	# Users	# Films	# Rating	# Rating range
MovieLens 100k	943	1682	10^5	1-5
MovieLens 1M	6040	3952	10^6	1-5

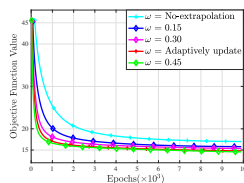
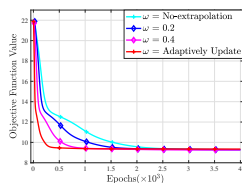
TABLE IV: NMAE(%) of recommender system on MovieLens 100k and MovieLens 1M datasets.

Dataset	$\rho(\%)$	IALM	NCARL	AEMC	DLMC	BiBNN	DNN-NSR
MovieLens 100k	30%	19.69	19.01	18.87	18.39	17.23	15.54
	50%	20.22	19.61	19.06	18.75	18.12	17.07
MovieLens 1M	30%	18.51	18.25	18.18	18.03	17.02	16.82
	50%	18.95	18.78	18.36	18.31	17.78	17.16

TABLE V: PSNRs for synthetic matrix $\mathbf{X} \in \mathbb{R}^{300 \times 200}$ with $\rho = 50\%$

and 80% and Images I in Fig. 1 with random masked pixels 40% and 50% for different values of μ_{\max} and $\mu_{\min} = 1$.

index	$\rho(\%)$	μ_{\max}						
		10^6	10^5	10^4	10^3	10^2	10	1
300×200	50	29.8678	27.5959	25.3325	20.5376	19.4572	17.4001	16.9405
	80	—	25.0967	22.1119	18.9528	16.1477	15.5734	14.1351
Image I	40	30.0741	27.7275	26.2802	24.2606	21.5966	20.2467	20.0874
	50	30.0301	27.0758	25.8667	24.1605	21.1786	20.1080	20.6373

(a) 300×200 synthesis matrix

(b) Image inpainting for Image I

Fig. 3: Variation of loss function for (a) 300×200 synthetic matrix with $\rho = 80\%$ and (b) Image I in Fig. 1 with $\rho = 50\%$.

nonsmooth regularization terms. We proved that the presented algorithm converges to critical points. We introduced the gradual addition of nonsmooth regularization terms and observed that it significantly affects performance. Simulation results on synthetic datasets, image inpainting, and recommender systems demonstrate the superiority of the proposed algorithm in comparison to previous methods.

VII. ACKNOWLEDGMENT

The last author was partially supported by the Research Foundation Flanders (FWO) grant G081222N and by the BOF DocPRO4 projects with ID 46929 and 48996.

APPENDIX A

PROOF OF PROPOSITION 1

By taking the partial derivatives of $g(\mathbf{h}_{1:n}^{(1:l)}, \mathbf{V}^{(1:l+1)}, \boldsymbol{\theta})$ with respect to $\mathbf{h}_q^{(i)}$ and $\mathbf{V}^{(j)}$, we get

$$\begin{aligned} \nabla_{\mathbf{h}_q^{(i)}} g(\mathbf{h}_q^{(<i)}, \mathbf{h}_q^{(i)}, \mathbf{h}_q^{(>i)}, \mathbf{V}^{(1:l+1)}, \boldsymbol{\theta}) &= \frac{1}{\mu_{\mathbf{h}^{(i)},k}} (\mathbf{h}_q^{(i)} - \mathbf{z}_q^{(i)}), \\ \nabla_{\mathbf{V}^{(j)}} g(\mathbf{h}_{1:n}^{(1:l)}, \mathbf{V}^{(<j)}, \mathbf{V}^{(j)}, \mathbf{V}^{(>j)}, \boldsymbol{\theta}) &= \frac{1}{\mu_{\mathbf{V}^{(j)},k}} (\mathbf{V}^{(j)} - \mathbf{W}^{(j)}), \end{aligned} \quad (57)$$

which are clearly Lipschitz continuous with moduli $L_{\mathbf{h}_q^{(i)},k} = \frac{1}{\mu_{\mathbf{h}^{(i)},k}}$ and $L_{\mathbf{V}^{(j)},k} = \frac{1}{\mu_{\mathbf{V}^{(j)},k}}$, respectively.

Since all activation functions are twice continuously differentiable, $g(\mathbf{h}_{1:n}^{(1:l)}, \mathbf{V}^{(1:l+1)}, \boldsymbol{\theta})$ is twice continuously differentiable with respect to $\boldsymbol{\theta}$. In addition, the set \mathcal{C} is compact. Therefore, invoking Lemma 4, there exists $L > 0$ such that the partial derivative of $g(\mathbf{h}_{1:n}^{(1:l)}, \mathbf{V}^{(1:l+1)}, \boldsymbol{\theta})$ with respect to $\boldsymbol{\theta}$ is L -Lipschitz continuous.

APPENDIX B

PROOF OF PROPOSITION 2

By fixing $\mathbf{h}_{1:n,k}^{(1:l)}$ and $\mathbf{V}_k^{(1:l+1)}$ and applying Lemma 5, we can write

$$\begin{aligned} g(\mathbf{h}_{1:n,k}^{(1:l)}, \mathbf{V}_k^{(1:l+1)}, \boldsymbol{\theta}_k) &\leq g(\mathbf{h}_{1:n,k}^{(1:l)}, \mathbf{V}_k^{(1:l+1)}, \boldsymbol{\theta}_{k-1}) + \\ \nabla_{\boldsymbol{\theta}}^T g(\mathbf{h}_{1:n,k}^{(1:l)}, \mathbf{V}_k^{(1:l+1)}, \boldsymbol{\theta}_{k-1}) &\left(\boldsymbol{\theta}_k - \boldsymbol{\theta}_{k-1} \right) + \frac{L_{\boldsymbol{\theta},k}}{2} \|\boldsymbol{\theta}_k - \boldsymbol{\theta}_{k-1}\|^2. \end{aligned} \quad (58)$$

Since $\boldsymbol{\theta}_k$ is the minimizer of (39), we obtain

$$\begin{aligned} & \nabla_{\boldsymbol{\theta}}^T g(\mathbf{h}_{1:n,k}^{(1:l)}, \mathbf{V}_k^{(1:l+1)}, \widehat{\boldsymbol{\theta}}_{k-1}) (\boldsymbol{\theta}_k - \widehat{\boldsymbol{\theta}}_{k-1}) + \frac{1}{2\mu_{\theta,k}} \|\boldsymbol{\theta}_k - \widehat{\boldsymbol{\theta}}_{k-1}\|^2 + r_{\theta}(\boldsymbol{\theta}_k) \\ & \leq \nabla_{\boldsymbol{\theta}}^T g(\mathbf{h}_{1:n,k}^{(1:l)}, \mathbf{V}_k^{(1:l+1)}, \widehat{\boldsymbol{\theta}}_{k-1}) (\boldsymbol{\theta}_k - \widehat{\boldsymbol{\theta}}_{k-1}) \\ & \quad - \widehat{\boldsymbol{\theta}}_{k-1}) + \frac{1}{2\mu_{\theta,k}} \|\boldsymbol{\theta}_k - \widehat{\boldsymbol{\theta}}_{k-1}\|^2 + r_{\theta}(\boldsymbol{\theta}_k). \end{aligned} \quad (59)$$

Summing the inequalities in (58) and (59) and adding and subtracting $\sum_{q=1}^n \sum_{i=1}^l r_h(\mathbf{h}_{q,k}^{(i)})$ and $\sum_{j=1}^{l+1} r_v(\mathbf{V}_k^{(j)})$ to the equation, we get

$$\begin{aligned} & \left[g(\mathbf{h}_{1:n,k}^{(1:l)}, \mathbf{V}_k^{(1:l+1)}, \boldsymbol{\theta}_{k-1}) + r_{\theta}(\boldsymbol{\theta}_{k-1}) + \sum_{q=1}^n \sum_{i=1}^l r_h(\mathbf{h}_{q,k}^{(i)}) + \sum_{j=1}^{l+1} r_v(\mathbf{V}_k^{(j)}) \right] \\ & - \left[g(\mathbf{h}_{1:n,k}^{(1:l)}, \mathbf{V}_k^{(1:l+1)}, \boldsymbol{\theta}_k) + r_{\theta}(\boldsymbol{\theta}_k) + \sum_{q=1}^n \sum_{i=1}^l r_h(\mathbf{h}_{q,k}^{(i)}) + \sum_{j=1}^{l+1} r_v(\mathbf{V}_k^{(j)}) \right] \geq \\ & \underbrace{\nabla_{\boldsymbol{\theta}}^T g(\mathbf{h}_{1:n,k}^{(1:l)}, \mathbf{V}_k^{(1:l+1)}, \widehat{\boldsymbol{\theta}}_{k-1}) (\boldsymbol{\theta}_k - \widehat{\boldsymbol{\theta}}_{k-1})}_{\text{I}} \\ & - \underbrace{\nabla_{\boldsymbol{\theta}}^T g(\mathbf{h}_{1:n,k}^{(1:l)}, \mathbf{V}_k^{(1:l+1)}, \widehat{\boldsymbol{\theta}}_{k-1}) (\boldsymbol{\theta}_{k-1} - \widehat{\boldsymbol{\theta}}_{k-1})}_{\text{II}} \\ & + \underbrace{\frac{1}{2\mu_{\theta,k}} \|\boldsymbol{\theta}_k - \widehat{\boldsymbol{\theta}}_{k-1}\|^2 - \frac{1}{2\mu_{\theta,k}} \|\boldsymbol{\theta}_{k-1} - \widehat{\boldsymbol{\theta}}_{k-1}\|^2 - \nabla_{\boldsymbol{\theta}}^T g(\mathbf{h}_{1:n,k}^{(1:l)}, \mathbf{V}_k^{(1:l+1)}, \boldsymbol{\theta}_{k-1}) (\boldsymbol{\theta}_k - \boldsymbol{\theta}_{k-1}) - \frac{L_{\theta,k}}{2} \|\boldsymbol{\theta}_k - \boldsymbol{\theta}_{k-1}\|^2}_{\text{III}}. \end{aligned} \quad (60)$$

Using (34), simplifying parts I and II, and invoking Lemma 6, III, it holds that

$$\begin{aligned} & Q(\mathbf{h}_{1:n,k}^{(1:l)}, \mathbf{V}_k^{(1:l+1)}, \boldsymbol{\theta}_{k-1}) - Q(\mathbf{h}_{1:n,k}^{(1:l)}, \mathbf{V}_k^{(1:l+1)}, \boldsymbol{\theta}_k) \geq \\ & \underbrace{\left[\nabla_{\boldsymbol{\theta}} g(\mathbf{h}_{1:n,k}^{(1:l)}, \mathbf{V}_k^{(1:l+1)}, \widehat{\boldsymbol{\theta}}_{k-1}) - \nabla_{\boldsymbol{\theta}} g(\mathbf{h}_{1:n,k}^{(1:l)}, \mathbf{V}_k^{(1:l+1)}, \boldsymbol{\theta}_{k-1}) \right]^T}_{\mathbf{u1}} \\ & \underbrace{(\boldsymbol{\theta}_k - \boldsymbol{\theta}_{k-1})}_{\mathbf{v1}} + \underbrace{\frac{1}{\mu_{\theta,k}} (\boldsymbol{\theta}_{k-1} - \widehat{\boldsymbol{\theta}}_{k-1})^T (\boldsymbol{\theta}_k - \boldsymbol{\theta}_{k-1})}_{\mathbf{u2}} \underbrace{(\boldsymbol{\theta}_k - \boldsymbol{\theta}_{k-1})}_{\mathbf{v2}} \\ & + \frac{1}{2\mu_{\theta,k}} \|\boldsymbol{\theta}_k - \boldsymbol{\theta}_{k-1}\|^2 - \frac{L_{\theta,k}}{2} \|\boldsymbol{\theta}_k - \boldsymbol{\theta}_{k-1}\|^2. \end{aligned} \quad (61)$$

Next, we apply the Cauchy-Schwartz inequality to the parts $\mathbf{u1} - \mathbf{v1}$ and $\mathbf{u2} - \mathbf{v2}$ in (61), i.e.,

$$\begin{aligned} \text{LHS} \geq & - \underbrace{\left\| \nabla_{\boldsymbol{\theta}} g(\mathbf{h}_{1:n,k}^{(1:l)}, \mathbf{V}_k^{(1:l+1)}, \widehat{\boldsymbol{\theta}}_{k-1}) - \nabla_{\boldsymbol{\theta}} g(\mathbf{h}_{1:n,k}^{(1:l)}, \mathbf{V}_k^{(1:l+1)}, \boldsymbol{\theta}_{k-1}) \right\|_2}_{\text{IV}} \end{aligned}$$

$$\begin{aligned} & + \frac{1}{\mu_{\theta,k}} \|\boldsymbol{\theta}_{k-1} - \widehat{\boldsymbol{\theta}}_{k-1}\| \left\| \boldsymbol{\theta}_k - \boldsymbol{\theta}_{k-1} \right\| + \left(\frac{1}{2\mu_{\theta,k}} - \frac{L_{\theta,k}}{2} \right) \|\boldsymbol{\theta}_k - \boldsymbol{\theta}_{k-1}\|^2 \\ & \geq - \underbrace{\left[L_{\theta,k} \|\boldsymbol{\theta}_{k-1} - \widehat{\boldsymbol{\theta}}_{k-1}\| + \frac{1}{\mu_{\theta,k}} \|\boldsymbol{\theta}_{k-1} - \widehat{\boldsymbol{\theta}}_{k-1}\| \right]}_{\text{VI}} \underbrace{\left\| \boldsymbol{\theta}_k - \boldsymbol{\theta}_{k-1} \right\|}_{\text{VI}} + \left(\frac{1}{2\mu_{\theta,k}} - \frac{L_{\theta,k}}{2} \right) \|\boldsymbol{\theta}_k - \boldsymbol{\theta}_{k-1}\|^2. \end{aligned} \quad (62)$$

From (40), we obtain $\|\boldsymbol{\theta}_{k-1} - \widehat{\boldsymbol{\theta}}_{k-1}\| = \omega_{\theta,k} \|\boldsymbol{\theta}_{k-1} - \boldsymbol{\theta}_{k-2}\|$, which consequently leads to

$$\begin{aligned} \text{LHS} \geq & - \left(L_{\theta,k} + \frac{1}{\mu_{\theta,k}} \right) \omega_{\theta,k} \|\boldsymbol{\theta}_{k-1} - \boldsymbol{\theta}_{k-2}\| \|\boldsymbol{\theta}_k - \boldsymbol{\theta}_{k-1}\| \\ & + \left(\frac{1}{2\mu_{\theta,k}} - \frac{L_{\theta,k}}{2} \right) \|\boldsymbol{\theta}_k - \boldsymbol{\theta}_{k-1}\|^2. \end{aligned} \quad (63)$$

Then, it follows from $\mu_{\theta,k} = \frac{1}{\gamma L_{\theta,k}}$ for $\gamma > 1$ that

$$\begin{aligned} \text{LHS} \geq & - (\gamma + 1) L_{\theta,k} \omega_{\theta,k} \|\boldsymbol{\theta}_{k-1} - \boldsymbol{\theta}_{k-2}\| \|\boldsymbol{\theta}_k - \boldsymbol{\theta}_{k-1}\| \\ & + \frac{(\gamma - 1) L_{\theta,k}}{2} \|\boldsymbol{\theta}_k - \boldsymbol{\theta}_{k-1}\|^2. \end{aligned} \quad (64)$$

On the other hand, setting $a = (\gamma + 1) L_{\theta,k} \omega_{\theta,k} \|\boldsymbol{\theta}_{k-1} - \boldsymbol{\theta}_{k-2}\|$ and $b = \|\boldsymbol{\theta}_k - \boldsymbol{\theta}_{k-1}\|$ and $\epsilon = \frac{(\gamma - 1) L_{\theta,k}}{2}$ and applying Lemma 7 imply

$$\begin{aligned} & Q(\mathbf{h}_{1:n,k}^{(1:l)}, \mathbf{V}_k^{(1:l+1)}, \boldsymbol{\theta}_{k-1}) - Q(\mathbf{h}_{1:n,k}^{(1:l)}, \mathbf{V}_k^{(1:l+1)}, \boldsymbol{\theta}_k) \geq - \\ & \frac{(\gamma + 1)^2 L_{\theta,k} \omega_{\theta,k}^2}{\gamma - 1} \|\boldsymbol{\theta}_{k-1} - \boldsymbol{\theta}_{k-2}\|^2 + \frac{(\gamma - 1) L_{\theta,k}}{4} \|\boldsymbol{\theta}_k - \boldsymbol{\theta}_{k-1}\|^2. \end{aligned} \quad (65)$$

Following the same procedure as in (58) and (59) for the subproblems (35a) and (35b), we end up with

$$\begin{aligned} & g(\mathbf{h}_{1:q-1,k}^{(1:l)}, \mathbf{h}_{q,k}^{(<i)}, \mathbf{h}_{q,k}^{(i)}, \mathbf{h}_{q,k-1}^{(>i)}, \mathbf{h}_{q+1:n,k-1}^{(1:l)}, \mathbf{V}_{k-1}^{(1:l+1)}, \boldsymbol{\theta}_{k-1}) \\ & + r_{h^{(i)}}(\mathbf{h}_{q,k}^{(i)}) + a_i \|\mathbf{h}_{q,k}^{(i)} - \mathbf{h}_{q,k-1}^{(i)}\|^2 \leq \\ & g(\mathbf{h}_{1:q-1,k}^{(1:l)}, \mathbf{h}_{q,k}^{(<i)}, \mathbf{h}_{q,k}^{(i)}, \mathbf{h}_{q,k-1}^{(>i)}, \mathbf{h}_{q+1:n,k-1}^{(1:l)}, \mathbf{V}_{k-1}^{(1:l+1)}, \boldsymbol{\theta}_{k-1}) \\ & + r_{h^{(i)}}(\mathbf{h}_{q,k-1}^{(i)}) \end{aligned} \quad (66)$$

and

$$\begin{aligned} & g(\mathbf{h}_{1:n,k}^{(1:l)}, \mathbf{V}_k^{(<j)}, \mathbf{V}_k^{(j)}, \mathbf{V}_{k-1}^{(>j)}, \boldsymbol{\theta}_{k-1}) + r_{v^{(j)}}(\mathbf{V}_k^{(j)}) \\ & b_i \|\mathbf{V}_k^{(j)} - \mathbf{V}_{k-1}^{(j)}\|_{\mathbb{F}}^2 \leq \end{aligned} \quad (67)$$

$$g(\mathbf{h}_{1:n,k}^{(1:l)}, \mathbf{V}_k^{(<j)}, \mathbf{V}_{k-1}^{(j)}, \mathbf{V}_{k-1}^{(>j)}, \boldsymbol{\theta}_{k-1}) + r_{v^{(j)}}(\mathbf{V}_{k-1}^{(j)}).$$

where the identities

$$a_i = \left(\frac{1}{2\mu_{h^{(i)},k}} - \frac{L_{h^{(i)},k}}{2} \right) = \frac{(\gamma - 1) L_{h^{(i)},k}}{2} > 0, \quad \gamma > 1,$$

$$b_j = \left(\frac{1}{2\mu_{v^{(j)},k}} - \frac{L_{v^{(j)},k}}{2} \right) = \frac{(\gamma-1)L_{v^{(j)},k}}{2} > 0, \quad \gamma > 1, \quad (68)$$

since $\mu_{h^{(i)},k} = \frac{1}{\gamma L_{h^{(i)},k}}$ (for $i = 1, \dots, l$) and $\mu_{v^{(j)},k} = \frac{1}{\gamma L_{v^{(j)},k}}$ (for $j = 1, \dots, l+1$). Now, fixing θ , writing (66) and (67) for $\mathbf{h}_1^{(1)}, \dots, \mathbf{h}_1^{(l)}, \dots, \mathbf{h}_n^{(1)}, \dots, \mathbf{h}_n^{(l)}, \mathbf{V}^{(1)}, \dots, \mathbf{V}^{(l+1)}$ respectively, and adding all the resulting inequalities, we consequently come to

$$\begin{aligned} & g(\mathbf{h}_{1:n,k}^{(1:l)}, \mathbf{V}_k^{(1:l+1)}, \boldsymbol{\theta}_{k-1}) + \sum_{q=1}^n \sum_{i=1}^l r_{h^{(i)}}(\mathbf{h}_{q,k}^{(i)}) \\ & + \sum_{j=1}^{l+1} r_{v^{(j)}}(\mathbf{V}_k^{(j)}) + \sum_{q=1}^n \sum_{i=1}^l a_i \|\mathbf{h}_{q,k}^{(i)} - \mathbf{h}_{q,k-1}^{(i)}\|^2 \\ & + \sum_{j=1}^{l+1} b_j \|\mathbf{V}_k^{(j)} - \mathbf{V}_{k-1}^{(j)}\|_F^2 + r_\theta(\boldsymbol{\theta}_{k-1}) \leq \quad (69) \\ & g(\mathbf{h}_{1:n,k-1}^{(1:l)}, \mathbf{V}_{k-1}^{(1:l+1)}, \boldsymbol{\theta}_{k-1}) + \sum_{q=1}^n \sum_{i=1}^l r_{h^{(i)}}(\mathbf{h}_{q,k-1}^{(i)}) \\ & + \sum_{j=1}^{l+1} r_{v^{(j)}}(\mathbf{V}_{k-1}^{(j)}) + r_\theta(\boldsymbol{\theta}_{k-1}). \end{aligned}$$

Added $r_\theta(\boldsymbol{\theta}_{k-1})$ to the both sides of (69) and using (34), the equation (69) can be rewritten as

$$\begin{aligned} & Q(\mathbf{h}_{1:n,k-1}^{(1:l)}, \mathbf{V}_{k-1}^{(1:l+1)}, \boldsymbol{\theta}_{k-1}) - Q(\mathbf{h}_{1:n,k}^{(1:l)}, \mathbf{V}_k^{(1:l+1)}, \boldsymbol{\theta}_{k-1}) \geq \\ & \sum_{q=1}^n \sum_{i=1}^l a_i \|\mathbf{h}_{q,k}^{(i)} - \mathbf{h}_{q,k-1}^{(i)}\|^2 + \sum_{j=1}^{l+1} b_j \|\mathbf{V}_k^{(j)} - \mathbf{V}_{k-1}^{(j)}\|_F^2. \quad (70) \end{aligned}$$

Summing up both sides of (65) and (70) leads to

$$\begin{aligned} & Q(\mathbf{h}_{1:n,k-1}^{(1:l)}, \mathbf{V}_{k-1}^{(1:l+1)}, \boldsymbol{\theta}_{k-1}) - Q(\mathbf{h}_{1:n,k}^{(1:l)}, \mathbf{V}_k^{(1:l+1)}, \boldsymbol{\theta}_k) \geq - \\ & \frac{(\gamma+1)^2 L_{\theta,k} \omega_{\theta,k}^2}{\gamma-1} \|\boldsymbol{\theta}_{k-1} - \boldsymbol{\theta}_{k-2}\|^2 + \frac{(\gamma-1)L_{\theta,k}}{4} \|\boldsymbol{\theta}_k - \boldsymbol{\theta}_{k-1}\|^2 \\ & + \sum_{q=1}^n \sum_{i=1}^l a_i \|\mathbf{h}_{q,k}^{(i)} - \mathbf{h}_{q,k-1}^{(i)}\|^2 + \sum_{j=1}^{l+1} b_j \|\mathbf{V}_k^{(j)} - \mathbf{V}_{k-1}^{(j)}\|_F^2. \quad (71) \end{aligned}$$

Using $\omega_{\theta,k} \leq \frac{\gamma-1}{2(\gamma+1)} \sqrt{\delta_k \frac{L_{\theta,k-1}}{L_{\theta,k}}}$ for $\delta_k < 1$, inequality (71) can be rewritten as

$$\begin{aligned} & Q(\mathbf{h}_{1:n,k-1}^{(1:l)}, \mathbf{V}_{k-1}^{(1:l+1)}, \boldsymbol{\theta}_{k-1}) - Q(\mathbf{h}_{1:n,k}^{(1:l)}, \mathbf{V}_k^{(1:l+1)}, \boldsymbol{\theta}_k) \geq - \\ & \frac{\delta_k(\gamma-1)L_{\theta,k-1}}{4} \|\boldsymbol{\theta}_{k-1} - \boldsymbol{\theta}_{k-2}\|^2 + \frac{(\gamma-1)L_{\theta,k}}{4} \|\boldsymbol{\theta}_k - \boldsymbol{\theta}_{k-1}\|^2 \\ & + \sum_{q=1}^n \sum_{i=1}^l a_i \|\mathbf{h}_{q,k}^{(i)} - \mathbf{h}_{q,k-1}^{(i)}\|^2 + \sum_{j=1}^{l+1} b_j \|\mathbf{V}_k^{(j)} - \mathbf{V}_{k-1}^{(j)}\|_F^2. \quad (72) \end{aligned}$$

Summing up both sides of this inequality from 1 to K , it holds

that

$$\begin{aligned} & Q(\mathbf{h}_{1:n,0}^{(1:l)}, \mathbf{V}_0^{(1:l+1)}, \boldsymbol{\theta}_0) - Q(\mathbf{h}_{1:n,K}^{(1:l)}, \mathbf{V}_K^{(1:l+1)}, \boldsymbol{\theta}_K) \geq \\ & \sum_{k=1}^{K-1} \frac{(1-\delta_{k+1})(\gamma-1)L_{\theta,k}}{4} \|\boldsymbol{\theta}_k - \boldsymbol{\theta}_{k-1}\|^2 + \frac{(\gamma-1)L_{\theta,k}}{4} \\ & \|\boldsymbol{\theta}_K - \boldsymbol{\theta}_{K-1}\|^2 - \frac{\delta_1(\gamma-1)L_{\theta,0}}{4} \|\boldsymbol{\theta}_0 - \boldsymbol{\theta}_{-1}\|^2 + \sum_{k=1}^K \sum_{q=1}^n \sum_{i=1}^l \\ & a_i \|\mathbf{h}_{q,k}^{(i)} - \mathbf{h}_{q,k-1}^{(i)}\|^2 + \sum_{k=1}^K \sum_{j=1}^{l+1} b_j \|\mathbf{V}_k^{(j)} - \mathbf{V}_{k-1}^{(j)}\|_F^2. \quad (73) \end{aligned}$$

Since $\boldsymbol{\theta}_0 = \boldsymbol{\theta}_{-1}$, we end up with

$$\begin{aligned} & Q(\mathbf{h}_{1:n,0}^{(1:l)}, \mathbf{V}_0^{(1:l+1)}, \boldsymbol{\theta}_0) - Q(\mathbf{h}_{1:n,K}^{(1:l)}, \mathbf{V}_K^{(1:l+1)}, \boldsymbol{\theta}_K) \geq \\ & \sum_{k=1}^K \frac{(1-\delta_{k+1})(\gamma-1)L_{\theta,k}}{4} \|\boldsymbol{\theta}_k - \boldsymbol{\theta}_{k-1}\|^2 + \sum_{k=1}^K \sum_{q=1}^n \sum_{i=1}^l \\ & a_i \|\mathbf{h}_{q,k}^{(i)} - \mathbf{h}_{q,k-1}^{(i)}\|^2 + \sum_{k=1}^K \sum_{j=1}^{l+1} b_j \|\mathbf{V}_k^{(j)} - \mathbf{V}_{k-1}^{(j)}\|_F^2, \quad (74) \end{aligned}$$

which guarantees

$$Q(\mathbf{h}_{1:n,K}^{(1:l)}, \mathbf{V}_K^{(1:l+1)}, \boldsymbol{\theta}_K) \leq Q(\mathbf{h}_{1:n,0}^{(1:l)}, \mathbf{V}_0^{(1:l+1)}, \boldsymbol{\theta}_0). \quad (75)$$

Letting $K \rightarrow \infty$ in this inequality, it can be deduced

$$\begin{aligned} & \sum_{k=1}^K \sum_{q=1}^n \sum_{i=1}^l a_i \|\mathbf{h}_{q,k}^{(i)} - \mathbf{h}_{q,k-1}^{(i)}\|^2 + \sum_{k=1}^K \sum_{j=1}^{l+1} b_j \|\mathbf{V}_k^{(j)} - \mathbf{V}_{k-1}^{(j)}\|_F^2 \\ & + \sum_{k=1}^K \frac{(1-\delta_{k+1})(\gamma-1)L_{\theta,k}}{4} \|\boldsymbol{\theta}_k - \boldsymbol{\theta}_{k-1}\|^2 \leq \infty, \quad (76) \end{aligned}$$

which leads to our desired results.

APPENDIX C

PROOF OF PROPOSITION 3

It follows from the inequality (75) that

$$\left(\{\mathbf{h}_k^{(i)}\}_{i=1}^l, \{\mathbf{V}_k^{(j)}\}_{j=1}^{l+1}, \boldsymbol{\theta}_k \right) \in \mathcal{L}_Q \left(\{\mathbf{h}_0^{(i)}\}_{i=1}^l, \{\mathbf{V}_0^{(j)}\}_{j=1}^{l+1}, \boldsymbol{\theta}_0 \right), \quad (77)$$

for the sublevel set

$$\begin{aligned} & \mathcal{L}_Q \left(\{\mathbf{h}_0^{(i)}\}_{i=1}^l, \{\mathbf{V}_0^{(j)}\}_{j=1}^{l+1}, \boldsymbol{\theta}_0 \right) = \{ (\{\mathbf{h}_k^{(i)}\}_{i=1}^l, \{\mathbf{V}_k^{(j)}\}_{j=1}^{l+1}, \boldsymbol{\theta}_k) : \\ & Q(\{\mathbf{h}_k^{(i)}\}_{i=1}^l, \{\mathbf{V}_k^{(j)}\}_{j=1}^{l+1}, \boldsymbol{\theta}_k) \leq Q(\{\mathbf{h}_0^{(i)}\}_{i=1}^l, \{\mathbf{V}_0^{(j)}\}_{j=1}^{l+1}, \boldsymbol{\theta}_0) \}. \quad (78) \end{aligned}$$

This clearly implies

$$\left\{ \{\mathbf{h}_k^{(i)}\}_{i=1}^l, \{\mathbf{V}_k^{(j)}\}_{j=1}^{l+1}, \boldsymbol{\theta}_k \right\} \subseteq \mathcal{L}_Q \left(\{\mathbf{h}_0^{(i)}\}_{i=1}^l, \{\mathbf{V}_0^{(j)}\}_{j=1}^{l+1}, \boldsymbol{\theta}_0 \right). \quad (79)$$

Therefore, its boundedness is followed by the boundedness of the lower level set.

APPENDIX D

PROOF OF THEOREM 1

- (a) In Proposition 3, we showed that the sequence $\{\{\mathbf{h}_k^{(i)}\}_{i=1}^l, \{\mathbf{V}_k^{(j)}\}_{j=1}^{l+1}, \boldsymbol{\theta}_k\}_{k \in \mathcal{I}}$ is bounded. The Bolzano-Weierstrass theorem [60] guarantees that a bounded sequence contains finite limit points.
- (b) If $\bar{\boldsymbol{\theta}}$ is a limit point of $\{\boldsymbol{\theta}_k\}$, then there exists a subsequence $\{\boldsymbol{\theta}_k\}_{k \in \mathcal{I}}$ converging to $\bar{\boldsymbol{\theta}}$. From Proposition 2, we have $\|\boldsymbol{\theta}_{k+1} - \boldsymbol{\theta}_k\|_2 \rightarrow 0$, i.e., for any $\gamma \geq 0$, $\{\boldsymbol{\theta}_{k+\gamma}\} \rightarrow \bar{\boldsymbol{\theta}}$. It follows from (39) that

$$\begin{aligned} & \underbrace{\nabla_{\boldsymbol{\theta}}^T g(\mathbf{h}_k^{(1:l)}, \mathbf{V}_k^{(1:l+1)}, \boldsymbol{\theta}_k)}_{\text{I}} (\boldsymbol{\theta}_k - \hat{\boldsymbol{\theta}}_{k-1}) + \underbrace{\frac{1}{2\mu_{\theta,k}} \|\boldsymbol{\theta}_k - \hat{\boldsymbol{\theta}}_{k-1}\|^2}_{\text{II}} \\ & + r_{\theta}(\boldsymbol{\theta}_k) \leq \nabla_{\boldsymbol{\theta}}^T g(\mathbf{h}_k^{(1:l)}, \mathbf{V}_k^{(1:l+1)}, \hat{\boldsymbol{\theta}}_{k-1}) (\boldsymbol{\theta} - \hat{\boldsymbol{\theta}}_{k-1}) \\ & + \frac{1}{2\mu_{\theta,k}} \|\boldsymbol{\theta} - \hat{\boldsymbol{\theta}}_{k-1}\|^2 + r_{\theta}(\boldsymbol{\theta}). \end{aligned} \quad (80)$$

Taking the limit from both sides of this inequality with $\mathcal{I} \ni k \rightarrow \infty$, the terms I and II tend to zero, i.e.,

$$\begin{aligned} \lim_{\mathcal{I} \ni k \rightarrow \infty} r_{\theta}(\boldsymbol{\theta}_k) & \leq \nabla_{\bar{\boldsymbol{\theta}}}^T g(\bar{\mathbf{h}}^{(1:l)}, \bar{\mathbf{V}}^{(1:l+1)}, \bar{\boldsymbol{\theta}}) (\boldsymbol{\theta} - \bar{\boldsymbol{\theta}}) \\ & + \frac{1}{2\bar{\mu}_{\theta}} \|\boldsymbol{\theta} - \bar{\boldsymbol{\theta}}\|^2 + r_{\theta}(\boldsymbol{\theta}), \end{aligned} \quad (81)$$

where $\bar{\mu}_{\theta}$ is a constant in the interval $(0, 1/\bar{L}_{\theta}]$, and \bar{L}_{θ} is the Lipschitz constant of $\nabla_{\boldsymbol{\theta}}^T g(\mathbf{h}^{(1:l)}, \mathbf{V}^{(1:l+1)}, \boldsymbol{\theta})$ at $\boldsymbol{\theta} = \bar{\boldsymbol{\theta}}$. Setting $\boldsymbol{\theta} = \bar{\boldsymbol{\theta}}$ in (81) leads to

$$\lim_{\mathcal{I} \ni k \rightarrow \infty} r_{\theta}(\boldsymbol{\theta}_k) \leq r_{\theta}(\bar{\boldsymbol{\theta}}). \quad (82)$$

On the other hand, $r_{\theta}(\boldsymbol{\theta})$ is lower semi-continuous [38], i.e.,

$$\lim_{\mathcal{I} \ni k \rightarrow \infty} r_{\theta}(\boldsymbol{\theta}_k) \geq r_{\theta}(\bar{\boldsymbol{\theta}}), \quad (83)$$

leading to

$$\lim_{\mathcal{I} \ni k \rightarrow \infty} r_{\theta}(\boldsymbol{\theta}_k) = r_{\theta}(\bar{\boldsymbol{\theta}}). \quad (84)$$

Since ℓ_1 and nuclear norm regularizers ($r_h(\mathbf{h}_q^{(i)})$ and $r_v(\mathbf{V}^{(j)})$) are lower semi-continuous [61], the first $2l+1$ regularization terms in (35a) and (35b) are lower semi-continuous. As such, the proof is similar for all other regularization terms.

- (c) By (81) and Assertion (b), we can write

$$\begin{aligned} \bar{\boldsymbol{\theta}} & = \arg \min_{\boldsymbol{\theta}} \nabla_{\boldsymbol{\theta}}^T g(\bar{\mathbf{h}}^{(1:l)}, \bar{\mathbf{V}}^{(1:l+1)}, \bar{\boldsymbol{\theta}}) (\boldsymbol{\theta} - \bar{\boldsymbol{\theta}}) \\ & + \frac{1}{2\bar{\mu}_{\theta}} \|\boldsymbol{\theta} - \bar{\boldsymbol{\theta}}\|^2 + r_{\theta}(\boldsymbol{\theta}). \end{aligned} \quad (85)$$

Thus, the first-order optimality condition is met for the objective function in (85) at $\boldsymbol{\theta} = \bar{\boldsymbol{\theta}}$, and we have

$$\mathbf{0} \in \nabla_{\theta} g(\bar{\boldsymbol{\theta}}) + \partial r_{\theta}(\bar{\boldsymbol{\theta}}). \quad (86)$$

Using (85) and (86), it is readily proved that $\{\bar{\boldsymbol{\theta}}\}$ is a

critical point of the objective function defined in (34). This process is similar for both $\mathbf{h}^{(1:l)}$ and $\mathbf{V}^{(1:l+1)}$.

- (d) Using Assertion (b), along with the continuity of $g(\mathbf{h}_{1:n}^{(1:l)}, \mathbf{V}^{(1:l+1)}, \boldsymbol{\theta})$, it can be deduced

$$\begin{aligned} & \lim_{\mathcal{I} \ni k \rightarrow \infty} Q(\mathbf{h}_k^{(1:l)}, \mathbf{V}_k^{(1:l+1)}, \boldsymbol{\theta}_k) = \\ & \lim_{\mathcal{I} \ni k \rightarrow \infty} g(\mathbf{h}_k^{(1:l)}, \mathbf{V}_k^{(1:l+1)}, \boldsymbol{\theta}_k) + \lim_{\mathcal{I} \ni k \rightarrow \infty} r_{\theta}(\boldsymbol{\theta}_k) = \\ & g(\bar{\mathbf{h}}^{(1:l)}, \bar{\mathbf{V}}^{(1:l+1)}, \bar{\boldsymbol{\theta}}) + r_{\theta}(\bar{\boldsymbol{\theta}}) = Q(\bar{\mathbf{h}}^{(1:l)}, \bar{\mathbf{V}}^{(1:l+1)}, \bar{\boldsymbol{\theta}}), \end{aligned} \quad (87)$$

which completes the proof.

REFERENCES

- [1] E. J. Candès and B. Recht, "Exact matrix completion via convex optimization," *Foundations of Computational mathematics*, vol. 9, no. 6, pp. 717–772, 2009.
- [2] E. J. Candès and T. Tao, "The power of convex relaxation: Near-optimal matrix completion," *IEEE Transactions on Information Theory*, vol. 56, no. 5, pp. 2053–2080, 2010.
- [3] G. Liu and P. Li, "Low-rank matrix completion in the presence of high coherence," *IEEE Transactions on Signal Processing*, vol. 64, no. 21, pp. 5623–5633, 2016.
- [4] X. Li, H. Zhang, and R. Zhang, "Matrix completion via non-convex relaxation and adaptive correlation learning," *IEEE Transactions on Pattern Analysis and Machine Intelligence*, 2022.
- [5] J. Fan and T. W. Chow, "Non-linear matrix completion," *Pattern Recognition*, vol. 77, pp. 378–394, 2018.
- [6] J. Fan and T. Chow, "Deep learning based matrix completion," *Neuro-computing*, vol. 266, pp. 540–549, 2017.
- [7] C. Guillemot and O. Le Meur, "Image inpainting: Overview and recent advances," *IEEE signal processing magazine*, vol. 31, no. 1, pp. 127–144, 2013.
- [8] M. Le Pendu, X. Jiang, and C. Guillemot, "Light field inpainting propagation via low rank matrix completion," *IEEE Transactions on Image Processing*, vol. 27, no. 4, pp. 1981–1993, 2018.
- [9] F. Xiao, W. Liu, Z. Li, L. Chen, and R. Wang, "Noise-tolerant wireless sensor networks localization via multinorms regularized matrix completion," *IEEE Transactions on Vehicular Technology*, vol. 67, no. 3, pp. 2409–2419, 2017.
- [10] T. L. Nguyen and Y. Shin, "Matrix completion optimization for localization in wireless sensor networks for intelligent iot," *Sensors*, vol. 16, no. 5, p. 722, 2016.
- [11] H. Steck, "Training and testing of recommender systems on data missing not at random," in *Proceedings of the 16th ACM SIGKDD international conference on Knowledge discovery and data mining*, 2010, pp. 713–722.
- [12] Y. Koren, "Factorization meets the neighborhood: a multifaceted collaborative filtering model," in *Proceedings of the 14th ACM SIGKDD international conference on Knowledge discovery and data mining*, 2008, pp. 426–434.
- [13] B. Recht, M. Fazel, and P. A. Parrilo, "Guaranteed minimum-rank solutions of linear matrix equations via nuclear norm minimization," *SIAM review*, vol. 52, no. 3, pp. 471–501, 2010.
- [14] J.-F. Cai, E. J. Candès, and Z. Shen, "A singular value thresholding algorithm for matrix completion," *SIAM Journal on optimization*, vol. 20, no. 4, pp. 1956–1982, 2010.
- [15] Z. Lin, M. Chen, and Y. Ma, "The augmented lagrange multiplier method for exact recovery of corrupted low-rank matrices," *arXiv preprint arXiv:1009.5055*, 2010.
- [16] Y. Hu, D. Zhang, J. Ye, X. Li, and X. He, "Fast and accurate matrix completion via truncated nuclear norm regularization," *IEEE transactions on pattern analysis and machine intelligence*, vol. 35, no. 9, pp. 2117–2130, 2012.
- [17] Q. Liu, Z. Lai, Z. Zhou, F. Kuang, and Z. Jin, "A truncated nuclear norm regularization method based on weighted residual error for matrix completion," *IEEE Transactions on Image Processing*, vol. 25, no. 1, pp. 316–330, 2015.
- [18] F. Nie, H. Huang, and C. Ding, "Low-rank matrix recovery via efficient Schatten p-norm minimization," in *Twenty-sixth AAAI conference on artificial intelligence*, 2012.

- [19] K.-C. Toh and S. Yun, "An accelerated proximal gradient algorithm for nuclear norm regularized linear least squares problems," *Pacific Journal of optimization*, vol. 6, no. 615-640, p. 15, 2010.
- [20] K. Mohan and M. Fazel, "Iterative reweighted algorithms for matrix rank minimization," *The Journal of Machine Learning Research*, vol. 13, no. 1, pp. 3441-3473, 2012.
- [21] N. Srebro, J. Rennie, and T. Jaakkola, "Maximum-margin matrix factorization," *Advances in neural information processing systems*, vol. 17, 2004.
- [22] J. D. Rennie and N. Srebro, "Fast maximum margin matrix factorization for collaborative prediction," in *Proceedings of the 22nd international conference on Machine learning*, 2005, pp. 713-719.
- [23] X. Li, H. Zhang, and R. Zhang, "Matrix completion via non-convex relaxation and adaptive correlation learning," *IEEE Transactions on Pattern Analysis and Machine Intelligence*, 2022.
- [24] Z. Wen, W. Yin, and Y. Zhang, "Solving a low-rank factorization model for matrix completion by a non-linear successive over-relaxation algorithm," *Mathematical Programming Computation*, vol. 4, no. 4, pp. 333-361, 2012.
- [25] E. J. Candès, X. Li, Y. Ma, and J. Wright, "Robust principal component analysis?" *Journal of the ACM (JACM)*, vol. 58, no. 3, pp. 1-37, 2011.
- [26] J. Fan and T. W. Chow, "Non-linear matrix completion," *Pattern Recognition*, vol. 77, pp. 378-394, 2018.
- [27] X. Hu, Y. Han, and Z. Geng, "A novel matrix completion model based on the multi-layer perceptron integrating kernel regularization," *IEEE Access*, vol. 9, pp. 67 042-67 050, 2021.
- [28] T. Zhou, H. Shan, A. Banerjee, and G. Sapiro, "Kernelized probabilistic matrix factorization: Exploiting graphs and side information," in *Proceedings of the 2012 SIAM international Conference on Data mining*. SIAM, 2012, pp. 403-414.
- [29] J. Fan and T. W. Chow, "Non-linear matrix completion," *Pattern Recognition*, vol. 77, pp. 378-394, 2018.
- [30] R. Salakhutdinov, A. Mnih, and G. Hinton, "Restricted boltzmann machines for collaborative filtering," in *Proceedings of the 24th international conference on Machine learning*, 2007, pp. 791-798.
- [31] S. Sedhain, A. K. Menon, S. Sanner, and L. Xie, "Autorec: Autoencoders meet collaborative filtering," in *Proceedings of the 24th international conference on World Wide Web*, 2015, pp. 111-112.
- [32] C.-Y. Wu, A. Ahmed, A. Beutel, A. J. Smola, and H. Jing, "Recurrent recommender networks," in *Proceedings of the tenth ACM international conference on web search and data mining*, 2017, pp. 495-503.
- [33] J. Fan and T. Chow, "Deep learning based matrix completion," *Neuro-computing*, vol. 266, pp. 540-549, 2017.
- [34] D. M. Nguyen, E. Tsiligianis, R. Calderbank, and N. Deligiannis, "Regularizing autoencoder-based matrix completion models via manifold learning," in *2018 26th European Signal Processing Conference (EUSIPCO)*. IEEE, 2018, pp. 1880-1884.
- [35] X. Hu, Y. Han, and Z. Geng, "A novel matrix completion model based on the multi-layer perceptron integrating kernel regularization," *IEEE Access*, vol. 9, pp. 67 042-67 050, 2021.
- [36] X. P. Li, M. Wang, and H. C. So, "An interpretable bi-branch neural network for matrix completion," *Signal Processing*, p. 108640, 2022.
- [37] S. Mehrdad and M. H. Kahaei, "Deep learning approach for matrix completion using manifold learning," *Signal Processing*, vol. 188, p. 108231, 2021.
- [38] S. Amini and S. Ghaemmaghami, "A new framework to train autoencoders through non-smooth regularization," *IEEE Transactions on Signal Processing*, vol. 67, no. 7, pp. 1860-1874, 2019.
- [39] S. Amini, M. Soltanian, M. Sadeghi, and S. Ghaemmaghami, "Non-smooth regularization: Improvement to learning framework through extrapolation," *IEEE Transactions on Signal Processing*, vol. 70, pp. 1213-1223, 2022.
- [40] Y. Xu and W. Yin, "A globally convergent algorithm for nonconvex optimization based on block coordinate update," *Journal of Scientific Computing*, vol. 72, no. 2, pp. 700-734, 2017.
- [41] N. Parikh, S. Boyd *et al.*, "Proximal algorithms," *Foundations and trends® in Optimization*, vol. 1, no. 3, pp. 127-239, 2014.
- [42] S. Amini and S. Ghaemmaghami, "Sparse autoencoders using non-smooth regularization," in *2018 26th European Signal Processing Conference (EUSIPCO)*. IEEE, 2018, pp. 2000-2004.
- [43] H. Attouch, J. Bolte, and B. F. Svaiter, "Convergence of descent methods for semi-algebraic and tame problems: proximal algorithms, forward-backward splitting, and regularized gauss-seidel methods," *Mathematical Programming*, vol. 137, no. 1-2, pp. 91-129, 2013.
- [44] W. H. Young, "On classes of summable functions and their fourier series," *Proceedings of the Royal Society of London. Series A, Containing Papers of a Mathematical and Physical Character*, vol. 87, no. 594, pp. 225-229, 1912.
- [45] J. Stewart, D. K. Clegg, and S. Watson, *Calculus: early transcendentals*. Cengage Learning, 2020.
- [46] H. Attouch, J. Bolte, P. Redont, and A. Soubeyran, "Proximal alternating minimization and projection methods for nonconvex problems: An approach based on the kurdyka-lojasiewicz inequality," *Mathematics of operations research*, vol. 35, no. 2, pp. 438-457, 2010.
- [47] J. Ba and R. Caruana, "Do deep nets really need to be deep?" *Advances in neural information processing systems*, vol. 27, 2014.
- [48] A. Golubeva, B. Neyshabur, and G. Gur-Ari, "Are wider nets better given the same number of parameters?" *arXiv preprint arXiv:2010.14495*, 2020.
- [49] H. Wang, S. Agarwal, and D. Papailiopoulos, "Pufferfish: communication-efficient models at no extra cost," *Proceedings of Machine Learning and Systems*, vol. 3, pp. 365-386, 2021.
- [50] Y. Xu and W. Yin, "A globally convergent algorithm for nonconvex optimization based on block coordinate update," *Journal of Scientific Computing*, vol. 72, no. 2, pp. 700-734, 2017.
- [51] Y. E. Nesterov, "A method of solving a convex programming problem with convergence rate $o(1/k^2)$," in *Doklady Akademii Nauk*, vol. 269, no. 3. Russian Academy of Sciences, 1983, pp. 543-547.
- [52] M. C. Mukkamala, F. Westerkamp, E. Laude, D. Cremers, and P. Ochs, "Bregman proximal framework for deep linear neural networks," *arXiv preprint arXiv:1910.03638*, 2019.
- [53] H. H. Bauschke, J. Bolte, and M. Teboulle, "A descent lemma beyond Lipschitz gradient continuity: first-order methods revisited and applications," *Mathematics of Operations Research*, vol. 42, no. 2, pp. 330-348, 2016.
- [54] H. Lu, R. M. Freund, and Y. Nesterov, "Relatively smooth convex optimization by first-order methods, and applications," *SIAM Journal on Optimization*, vol. 28, no. 1, pp. 333-354, 2018.
- [55] M. Ahooshoh, L. T. K. Hien, N. Gillis, and P. Patrinos, "Multi-block Bregman proximal alternating linearized minimization and its application to orthogonal nonnegative matrix factorization," *Computational Optimization and Applications*, vol. 79, no. 3, pp. 681-715, 2021.
- [56] M. Ahooshoh, L. T. K. Hien, N. Gillis, and P. Patrinos, "A block inertial Bregman proximal algorithm for nonsmooth nonconvex problems with application to symmetric nonnegative matrix tri-factorization," *Journal of Optimization Theory and Applications*, vol. 190, no. 1, pp. 234-258, 2021.
- [57] L. T. Khanh Hien, D. N. Phan, N. Gillis, M. Ahooshoh, and P. Patrinos, "Block Bregman majorization minimization with extrapolation," *SIAM Journal on Mathematics of Data Science*, vol. 4, no. 1, pp. 1-25, 2022.
- [58] J. Fan, M. Zhao, and T. W. Chow, "Matrix completion via sparse factorization solved by accelerated proximal alternating linearized minimization," *IEEE Transactions on Big Data*, vol. 6, no. 1, pp. 119-130, 2018.
- [59] H. Ye, H. Li, F. Cao, and L. Zhang, "A hybrid truncated norm regularization method for matrix completion," *IEEE Transactions on Image Processing*, vol. 28, no. 10, pp. 5171-5186, 2019.
- [60] Y. LeCun, L. Bottou, Y. Bengio, and P. Haffner, "Gradient-based learning applied to document recognition," *Proceedings of the IEEE*, vol. 86, no. 11, pp. 2278-2324, 1998.
- [61] J. Chong, "Math 742: Geometric analysis."